applied sciences

Article

Distributed Formation Control for Underactuated, Unmanned Surface Vehicles with Uncertainties and Disturbances

Wenbin Huang [1,2], Yuxin Zheng [3], Lei Zhang [3,*], Yanhao Li [3] and Xi Chen [2]

1 School of Marine Science and Technology, Northwestern Polytechnical University, Xi'an 710072, China; huangwenbin_cv@163.com
2 Marine Design & Research Institute of China, Shanghai 200011, China; chenxi77777778@163.com
3 National Key Laboratory of Autonomous Marine Vehicle Technology, Harbin Engineering University, Harbin 150001, China; zhengyuxin@hrbeu.edu.cn (Y.Z.); liyanhao@hrbeu.edu.cn (Y.L.)
* Correspondence: zhanglei103@hrbeu.edu.cn

Abstract: This paper investigates the distributed formation control problem of underactuated unmanned surface vehicles (UUSVs) with uncertainties and disturbances and proposes a novel distributed formation controller. The proposed controller redefines the dynamic and kinematic models for each UUSV, which reduces the complexity of the underactuated controller design. Dynamic surface control (DSC) is employed to eliminate the repeated derivatives of the virtual control law, which is crucial for the generation of real-time control signals. The proposed controller integrates neural network approximation with MLP-based adaptive laws to enhance the model's resistance to disturbances. Then, an auxiliary adaptive law is designed for each UUSV to obtain a continuous controller under the compensation of approximate errors and disturbances. The results demonstrate that the controller achieves the desired goals for the formation control, and all control signals are guaranteed to be semi-global uniformly ultimately bounded (SGUUB). The final simulation results thoroughly prove the effectiveness of the theoretical results.

Keywords: UUSV; distributed control; formation control; dynamic surface control

check for updates

Citation: Huang, W.; Zheng, Y.; Zhang, L.; Li, Y.; Chen, X. Distributed Formation Control for Underactuated, Unmanned Surface Vehicles with Uncertainties and Disturbances. *Appl. Sci.* **2024**, *14*, 12064. https://doi.org/10.3390/app142412064

Academic Editor: José A. Orosa

Received: 14 November 2024
Revised: 11 December 2024
Accepted: 16 December 2024
Published: 23 December 2024

1. Introduction

With the development of ocean engineering technology and the expansion of mission requirements in both military and civilian fields, the control of unmanned surface vehicle (USV) formation has received widespread attention in recent years. The cooperation of multiple USVs offers several advantages, including greater flexibility, adaptability, and higher performance. For instance, in maritime search and rescue operations, multiple USVs can achieve extensive coverage of the target area, completing the entire mission in less time. Other applications include marine mineral exploration, territorial sea monitoring, the escorting of vehicles, fire support, and anti-submarine operations [1–8].

For multi-vehicle formation cooperative systems, Li et al. [9] provided a novel adaptive fuzzy output regulation method to address the multi-vehicle formation problem. Firstly, a distributed observer was employed to obtain the feedforward information of the reference system, and, then, within the backstepping framework, a distributed adaptive fuzzy control law for USV formation was designed. Based on neurodynamical optimization and fuzzy approximation techniques, Peng et al. [10] have not only achieved formation keeping for multi-vehicle formation but also enabled flexible formation maneuvers. Peng et al. [11] designed an adaptive dynamic surface multi-vehicle formation control scheme for USV clusters with uncertain dynamics. Subsequently, they developed a neural network formation controller for USV clusters based on graph theory formation structures, which can handle two types of cooperative formation problems for USVs with uncertain dynamics, both in leaderless and leader-based scenarios [12]. He and Zhao et al. [6,13] studied the control problem of a group of fully actuated USVs with a decentralized leader–follower structure. He et al. [14] improved the formation control design of a multi-vehicle radial basis function (RBF) neural network by introducing a robust feedback term in the feedback control to compensate for the neural network approximation error and external disturbance, thus obtaining the asymptotic tracking performance of USV formation. Chen et al. [15] proposed an adaptive cooperative control law for USVs based on the adaptive backstepping method to estimate the reference orbiting velocity in bidirectional communication topology, thus eliminating the limitation that every vehicle must obtain the reference trajectory in the existing literature. Aiming at the parametric uncertainty of the USV model, a new adaptive fault-tolerant formation control scheme for USVs with a leader–follower structure was designed, which is suitable for the control of UUSV clusters with a partially known input gain function [16]. Riahifard et al. [17] provided a multi-vehicle adaptive formation control, which can solve the leader–follower formation problem of UUSV clusters with uncertain dynamics and input constraints. Qu et al. [18] proposed a nonlinear positioning control for the UUSV, which resists unknown disturbance through adaptive heading control. Karnani et al. [19] considered UUSV trajectory tracking, provided an optimal control strategy for the vehicle in the presence of external disturbance, and proposed a controller-based model reference adaptive control scheme with an integrator, ensuring the stability of closed-loop systems. Mu et al. [20] considered the trajectory tracking control problem of UUSVs affected by uncertain dynamics and input saturation. This paper uses first-order and second-order sliding mode surfaces to design an underactuated trajectory tracking controller. The auxiliary system solves the potential input saturation problem, uses the MLP method of the neural network to further reduce the computational burden of the controller, and further enhances the robustness of the trajectory tracking system by introducing an adaptive robust term.

On this basis, we further studied the distributed formation control problem of UUSVs with uncertainties and disturbances, in which UUSVs can communicate with each other under directed interaction topology. For each UUSV, a new distributed neural network formation controller with two adaptive laws is proposed. First, a virtual control law is established based on static consensus protocol and directed graph theory. Then, the formation controller is derived using DSC, and, then, the adaptive law based on MLP is used to deal with uncertain dynamics. When compensating for approximation errors and external disturbances, auxiliary control laws and corresponding adaptive laws are added to obtain a continuous controller.

The main contributions of this paper are summarized as follows:

(1) For the underactuated problem, the dynamic and kinematic models of the formation were transformed, redefined, and decomposed into the attitude subsystem and position subsystem, thereby achieving independent control of each degree of freedom of UUSVs.

(2) For the complex differential explosion problem caused by the virtual control law in the calculation process, DSC technology was adopted in the controller design to avoid the repeated differentiation of the virtual control law and reduce the computational complexity. At the same time, combining RBF neural network approximation with MLP-based adaptive law enhances the model's anti-disturbance ability.

The rest of this paper is organized as follows: Section 2 introduces the basic knowledge of graph theory and RBF neural networks. Section 3 introduces the design process of the cooperative formation controller. Section 4 conducts simulation. Section 5 summarizes this paper.

Notations: R^N represents the N-dimensional real number space, given the vector $\boldsymbol{x} = [x_1, \ldots, x_N]^{\mathrm{T}}$, $\|\boldsymbol{x}\|_1$ represents the 1-norm of $\boldsymbol{x}$, $\|\boldsymbol{x}\|_2$ represents the 2-norm of $\boldsymbol{x}$, and $\|\boldsymbol{x}\|_\infty$ represents the ∞-norm of $\boldsymbol{x}$. Define $\tanh(\boldsymbol{x}) = [\tanh(x_1), \cdots, \tanh(x_N)]^{\mathrm{T}}$. Define vector $\boldsymbol{h} = \left[\boldsymbol{h}_1^{\mathrm{T}}, \ldots, \boldsymbol{h}_N^{\mathrm{T}}\right]^{\mathrm{T}}$, where $\boldsymbol{h}_i$, $i = 1, \ldots, N$ is also a vector. Define $\boldsymbol{h} \circ \boldsymbol{h} = \left[\boldsymbol{h}_1^{\mathrm{T}}\boldsymbol{h}_1, \ldots, \boldsymbol{h}_N^{\mathrm{T}}\boldsymbol{h}_N\right]^{\mathrm{T}}$. $\boldsymbol{I}$ is a column vector with all elements being 1. $\boldsymbol{A}^{\mathrm{T}}$ represents the trans-position of matrix $\boldsymbol{A}$. $\lambda(\boldsymbol{A})$ represents the eigenvalues of matrix $\boldsymbol{A}$, $\boldsymbol{A} = \text{diag}\{\boldsymbol{A}_{11}, \ldots, \boldsymbol{A}_{NN}\}$ represents the extraction of diagonal elements in matrix $\boldsymbol{A}$. $\boldsymbol{A} \otimes \boldsymbol{B}$ represents the Kronecker product of matrices $\boldsymbol{A}$ and $\boldsymbol{B}$.

2. Related Works and Problem Statement

2.1. Graph Theory

In a directed graph $\mathcal{G}$, for a system containing N UUSVs, the information interaction model can be represented by the graph $\mathcal{G} = \{\mathcal{V}, \mathcal{E}, A\}$, where $\mathcal{V} = \{v_1, \cdots v_N\}$ represents the set of UUSVs, $\mathcal{E} \subseteq \mathcal{V} \times \mathcal{V}$ represents the set of edges between N UUSVs. If $(i,j) \in \mathcal{E}$, it means that UUSV i and UUSV j are adjacent (the neighbors of UUSV i are represented by N_i); that is, UUSV j is within the communication radius of UUSV i and can receive the signal sent by UUSV i. $A = [a_{ij}] \in \mathbb{R}^{N \times N}$ represents the adjacency matrix of the directed graph $\mathcal{G}$. Generally speaking, there are no self-loops in the graph $\mathcal{G}$; that is, edges (i,i) cannot appear. All the diagonal elements $a_{ii} = 0$ in A. $a_{ij} > 0$ indicates that UUSV i can send information to UUSV j through the edge (i,j); $a_{ij} = 0$ indicates that there is no path between UUSV i and j.

The value of element A in the adjacency matrix of directed graph $\mathcal{G}$ is as follows:

$$a_{ij} = \begin{cases} 1 & (i,j) \in \mathcal{E}, i \neq j \\ 0 & other \end{cases} \tag{1}$$

The Laplace matrix $\mathcal{L} \triangleq [l_{ij}] \in \mathbb{R}^{N \times N}$ of a directed graph $\mathcal{G}$ can be obtained from the adjacency matrix:

$$i_j = \begin{cases} \sum\limits_{j \in N_i} a_{ij}, i = j \\ -a_{ij}, i \neq j \end{cases} \tag{2}$$

Lemma 1 [21]**.** *If the interaction graph $\mathcal{G}$ contains at least one directed spanningtree, then its corresponding Laplacian matrix $\mathcal{L}$ is positive definite.*

2.2. Function Approximation Based on RBF Neural Network

Because of the special structure of the RBF neural network, it can approximate any continuous function. In this paper, the RBF neural network was used to approximate the unknown part of the UUSV mathematical model. The principle is as described in Lemma 2.

Lemma 2. *For a given arbitrary continuous function $f(t)$, there is an arbitrary network weight $\boldsymbol{W} = [w_1, \ldots, w_N]^T$, so that*

$$f(t) = \boldsymbol{W}^T \boldsymbol{h}(t) + \varepsilon \tag{3}$$

where t is the input vector, $\varepsilon$is the approximation error of RBF network, $\boldsymbol{h}(t)$ is the hidden layer of the network, and outputs the following equation:

$$\boldsymbol{h}_i(t) = \exp\left(-\frac{\|\boldsymbol{x}(t) - \boldsymbol{c}_i(t)\|_2^2}{2b_i^2}\right), i = 1, \cdots N \tag{4}$$

where b_i is a positive scalar representing the width of the i-th Gaussian basis function of the hidden layer; N is the number of hidden layer nodes.

2.3. Problem Statement

Considering the formation composed of N UUSVs, the kinematic and dynamic equations of UUSV i are described as

$$\begin{cases} \dot{\boldsymbol{P}}_i = \boldsymbol{J}_i(\theta_i)\boldsymbol{Q}_i \\ \dot{\theta}_i = r_i \end{cases} \tag{5}$$

$$\begin{cases} \dot{\boldsymbol{Q}}_i = \boldsymbol{F}_i(x_i, y_i) + \boldsymbol{\tau}_i^w + \boldsymbol{\tau}_i \\ \dot{r}_i = f_i(\sigma_i) + \frac{1}{m_i^{33}}\tau_i^{w\sigma} + \frac{1}{m_i^{33}}\tau_i^{\sigma} \end{cases} \tag{6}$$

where $i = 1, 2, \ldots, N$ represents the identification number of the UUSV, $\boldsymbol{P}_i = [x_i, y_i]^{\mathrm{T}}$ is the position vector of the UUSV in the earth coordinate system, (x_i, y_i) are the position coordinates; $\boldsymbol{J}_i(\theta_i) = \begin{bmatrix} \cos\theta_i & -\sin\theta_i \\ \sin\theta_i & \cos\theta_i \end{bmatrix}$ is the rotation matrix related to the yaw angle, θ_i is the yaw angle; $\boldsymbol{Q}_i = [u_i, v_i]^{\mathrm{T}}$ is the velocity vector in the hull coordinate system, with u_i and v_i representing the forward and lateral drift velocities, respectively, and r_i representing the yaw angular velocity of the UUSV. $\boldsymbol{F}_i(x_i, y_i) = [f_i(x_i), f_i(y_i)]^{\mathrm{T}}$ and $f_i(\sigma_i)$ denote the unknown unmodeled dynamics. $\boldsymbol{\tau}_i^w = \left[\frac{1}{m_i^{11}}\tau_i^{wX}, \frac{1}{m_i^{22}}\tau_i^{wY}\right]^{\mathrm{T}}$ and $\tau_i^{w\sigma}$ are the external disturbances of the UUSV, and $\boldsymbol{\tau}_i = \left[\frac{1}{m_i^{11}}\tau_i^{X}, 0\right]$ and τ_i^{σ} are the control inputs of the UUSV.

Since the above model is underactuated, $U_i = \sqrt{u_i^2 + v_i^2}$ is further defined as the resultant velocity, $u_i = U_i\cos\varphi_i$, φ_i is the sideslip angle, and $\varphi_i = \arctan\left(\frac{v_i}{u_i}\right)$, so the above dynamic model can be simplified as

$$\begin{cases} \dot{\boldsymbol{P}}_i = U_i\boldsymbol{R}_i(\theta_i) \\ \dot{\theta}_i = r_i \end{cases} \tag{7}$$

where $\boldsymbol{R}_i(\theta_i) = [\cos\theta_{iw}, \sin\theta_{iw}]^{\mathrm{T}}$. $\theta_{iw} = \theta_i + \varphi_i$ is the heading angle.

Since $u_i = U_i\cos\varphi_i$, it can be concluded that

$$\dot{u}_i = \dot{U}_i - 2\dot{U}_i\sin^2\left(\frac{\varphi_i}{2}\right) - \dot{U}_i\sin^2(\varphi_i)\dot{\varphi}_i \tag{8}$$

The kinetic equation can be further organized into the following form:

$$\begin{cases} \dot{U}_i = 2\dot{U}_i\sin^2\left(\frac{\varphi_i}{2}\right) + \dot{U}_i\sin^2(\varphi_i)\dot{\varphi}_i + f_i(x_i) + \frac{1}{m_i^{11}}\tau_i^{wX} + \frac{1}{m_i^{11}}\tau_i^{X} \\ \dot{r}_i = f_i(\sigma_i) + \frac{1}{m_i^{33}}\tau_i^{w\sigma} + \frac{1}{m_i^{33}}\tau_i^{\sigma} \end{cases} \tag{9}$$

For the convenience of further research, the UUSV model can be expressed as the attitude subsystem and position subsystem. Based on the previous derivation, the attitude subsystem and the position subsystem can be written as

$$\begin{cases} \dot{\theta}_i = r_i \\ \dot{r}_i = \frac{1}{m_i^{33}}\tau_i^{\sigma} + \overset{-\sigma}{\boldsymbol{f}_i} \end{cases} \tag{10}$$

where $\overset{-\sigma}{\boldsymbol{f}_i} = f_i(\sigma_i) + \frac{1}{m_i^{33}}\tau_i^{w\sigma}$.

$$\begin{cases} \dot{\boldsymbol{P}}_i = U_i\boldsymbol{R}_i(\theta_i) \\ \dot{U}_i = \frac{1}{m_i^{11}}\tau_i^{X} + \overset{-X}{\boldsymbol{f}_i} \end{cases} \tag{11}$$

where $\overset{-X}{\boldsymbol{f}_i} = 2\dot{U}_i \sin^2\left(\frac{\varphi_i}{2}\right) + \dot{U}_i \sin^2(\varphi_i)\dot{\varphi}_i + f_i(x_i) + \frac{1}{m_i^{11}}\tau_i^{wX}$, $\overset{-X}{\boldsymbol{f}_i} = 2\dot{U}_i \sin^2\left(\frac{\varphi_i}{2}\right) + \dot{U}_i \sin^2(\varphi_i)\dot{\varphi}_i + f_i(x_i) + \frac{1}{m_i^{11}}\tau_i^{wX}$; $\overset{-\sigma}{\boldsymbol{f}_i}$ and $\overset{-X}{\boldsymbol{f}_i}$ represent state-dependent nonlinearities, including unmodeled dynamics and external disturbances.

Remark 1. *Compared to fully actuated USVs, UUSVs are difficult to independently control all degrees of freedom through control inputs. Therefore, this paper solves this issue by performing the aforementioned transformations and redefinitions on the dynamic and kinematic models of the UUSVs. For multiple UUSVs, the system is described using (10), (11), and a directed graph $\mathcal{G}$. By relying on the state $(\theta_i, r_i, \boldsymbol{P}_i, U_i)$ of each UUSV and the state $\left(\theta_j, r_j, \boldsymbol{P}_j, U_j\right)$, $j \in N$ of its neighbors within the directed graph $\mathcal{G}$, the distributed control laws τ_i^X and τ_i^σ for each UUSV are designed using (10) and (11) to achieve the formation control of UUSVs.*

Control Objective: Considering a formation composed of N UUSVs, design a distributed adaptive controller under conditions of unknown model parameters and complex disturbances to achieve stable formation control.

Next, some important assumptions and lemmas are introduced for later use.

Assumption 1. *Considering the boundedness of the time-varying reference trajectory $\boldsymbol{r}_j$ and the expected velocity $\boldsymbol{U}_r$, there are positive constants ρ_M, $\rho_U \in R$ such that $\|\boldsymbol{r}_j\|_1 \leq \rho_M$, $\|\boldsymbol{U}_r\|_1 \leq \rho_U$.*

Assumption 2. *Considering the boundedness of external perturbation $\overset{-X}{\boldsymbol{f}_i}$, $\overset{-\sigma}{\boldsymbol{f}_i}$, there are positive constants $b_d^X, b_d \in \mathrm{R}$ such that $\left\|\overset{-X}{\boldsymbol{f}_i}\right\|_2 \leq b_d^X$, $\left\|\overset{-\sigma}{\boldsymbol{f}_i}\right\| \leq b_d$.*

Lemma 3. *The following inequality holds for any constant $\varepsilon > 0$ and any vector $x \in \mathrm{R}^{\mathrm{N}}$, where the constant $k_p = k_{p_1} = 0.2785$:*

$$\|x\|_\infty \leq k_p\varepsilon + x^{\mathrm{T}}\tanh\left(\frac{x}{\varepsilon}\right) \tag{12}$$

Lemma 4 [22]**.** *Given two vectors x,$y \in R^N$, there is the following inequality for any constant$\varepsilon > 0$:*

$$x^{\mathrm{T}}y \leq \frac{1}{2}(\varepsilon x^{\mathrm{T}}x + \frac{1}{\varepsilon}y^{\mathrm{T}}y) \tag{13}$$

Lemma 5 [23]**.** *Consider a system $\dot{\boldsymbol{x}} = f(\boldsymbol{x})$,$\boldsymbol{x} \in R^N$, for its bounded initial state $\boldsymbol{x}(0)$, if there exists a continuous positive definite Lyapunov function $V(\boldsymbol{x})$, $\kappa_1(\|\boldsymbol{x}\|) \leq V(\boldsymbol{x}) \leq \kappa_2(\|\boldsymbol{x}\|)$, and $\dot{V} \leq -\alpha V + \beta$, where $\kappa_1(\cdot)$ and $\kappa_2(\cdot)$ are the $\mathcal{K}$ function. α and β are positive constants. Then, its solution $\boldsymbol{x}$ is SGUUB.*

3. Controller Design

The adaptive controller design of multi-UUSVs is divided into two parts. First, the attitude subsystem is used to design the control law τ_i^σ for each UUSV, and, then, the position subsystem is used to design the control law τ_i^X for each UUSV. The specific design process is below.

3.1. Attitude Controller Design

For the attitude subsystem, define the error variables z_{i1}, z_{i2}, z_{i3} as follows:

$$\begin{cases} z_{i1} = \theta_i - \theta_j \\ z_{i2} = \overline{\alpha}_{i1} - \alpha_{i1} \\ z_{i3} = r_i - \overline{\alpha}_{i1} \end{cases} \tag{14}$$

where α_{i1} is a virtual control law. $\overline{\alpha}_{i1}$ is a filter control law. $\overline{\alpha}_{i1}$ is obtained by α_{i1} through a first-order filter. Time constant γ_i is given by the corresponding diagonal element and is a diagonal positive definite matrix.

$$\gamma_i \dot{\overline{\alpha}}_{i1} + \overline{\alpha}_{i1} = \alpha_{i1} \tag{15}$$

The derivative of the error variable z_{i1}, z_{i2}, z_{i3} can be obtained as follows:

$$\begin{cases} \dot{z}_{i1} = z_{i2} + z_{i3} + \alpha_{i1} - \dot{r}_j \\ \dot{z}_{i2} = -\gamma_i^{-1} z_{i2} \underset{-\sigma}{-} \dot{\alpha}_{i1} \\ \dot{z}_{i3} = \frac{1}{m_i^{33}} \tau_i^{\sigma} + \boldsymbol{f}_i + \gamma_i^{-1} z_{i2} \end{cases} \tag{16}$$

In this paper, DSC is adopted to deal with the complex differential problem in the calculation process of virtual control law α_{i1}, which further improves the practicability of the controller.

Firstly, a Lyapunov function is selected as follows:

$$V_1 = \frac{1}{2} z_1^{\mathrm{T}} z_1 \tag{17}$$

The derivative of V_1 with respect to time is

$$\dot{V}_1 = z_1^{\mathrm{T}} \left[z_2 + z_3 + \boldsymbol{\alpha_1} - \dot{\boldsymbol{r}}_j \right] \tag{18}$$

Construct the virtual control law as

$$\alpha_{i1} = -\boldsymbol{K}_{i1} z_{i1} - \boldsymbol{K}_{i0} \tanh\left(\frac{N z_{i1}}{\varepsilon} \right) \tag{19}$$

where $\boldsymbol{K}_{i1}$,$\boldsymbol{K}_{i0} \in \mathrm{R}^{3\times3}$ is a diagonal matrix. ε is a variable positive constant. Definition $z_1 = [z_{11}, \ldots, z_{N1}]^{\mathrm{T}}$, $z_2 = [z_{12}, \ldots, z_{N2}]^{\mathrm{T}}$, $z_3 = [z_{13}, \ldots, z_{N3}]^{\mathrm{T}}$, $\boldsymbol{K}_0 = \mathrm{diag}\{\boldsymbol{K}_{i0}\}$, $\boldsymbol{K}_1 = \mathrm{diag}\{\boldsymbol{K}_{i1}\}$, and $\boldsymbol{\gamma} = \mathrm{diag}\{\gamma_i\}$,$\alpha_1 = [\alpha_{i1}, \ldots, \alpha_{N1}]^{\mathrm{T}}$.

Therefore, the virtual control law α_{i1} can be written in the following form:

$$\boldsymbol{\alpha}_1 = -\boldsymbol{K}_1 z_1 - \boldsymbol{K}_0 \tanh\left(\frac{N z_1}{\varepsilon} \right) \tag{20}$$

Substituting (21) into (19),

$$\dot{V}_1 = z_1^{\boldsymbol{T}}(z_2 + z_3) - z_1^{\mathrm{T}} \boldsymbol{K}_1 z_1 - \boldsymbol{K}_0 z_1^{\mathrm{T}} \tanh\left(\frac{N z_1}{\varepsilon} \right) - z_1^{\mathrm{T}} \dot{\boldsymbol{r}}_j \tag{21}$$

According to Lemma 3, it can be obtained as follows:

$$\begin{aligned} \dot{V}_1 &\le z_1^{\mathrm{T}}(z_2 + z_3) - z_1^{\mathrm{T}} \boldsymbol{K}_1 z_1 - \boldsymbol{K}_0 z_1^{\mathrm{T}} \tanh\left(\tfrac{N z_1}{\varepsilon} \right) + \| z_1 \|_\infty N \rho_M \\ &\le z_1^{\mathrm{T}}(z_2 + z_3) - z_1^{\mathrm{T}} \boldsymbol{K}_1 z_1 - \boldsymbol{K}_0 z_1^{\mathrm{T}} \tanh\left(\tfrac{N z_1}{\varepsilon} \right) + N \rho_M k_p \varepsilon + N^2 \rho_M z_1^{\mathrm{T}} \tan\mathrm{h}\left(\tfrac{N z_1}{\varepsilon} \right) \end{aligned} \tag{22}$$

Let $\lambda(\boldsymbol{K}_0)_{\min} > N^2\rho_M$, and we can further conclude that $N^2\rho_M z_1^{\mathrm{T}}\tanh(\frac{Nz_1}{\varepsilon}) - \boldsymbol{K}_0 z_1^{\mathrm{T}}\tanh\left(\frac{Nz_1}{\varepsilon}\right) < 0$. Then, the derivative of V_1 satisfies

$$\dot{V}_1 \leq -z_1^{\mathrm{T}}\boldsymbol{K}_1 z_1 + z_1^{\mathrm{T}} z_2 + z_1^{\mathrm{T}} z_3 + N\rho_M k_p \varepsilon \tag{23}$$

Next, the attitude control law $\boldsymbol{\tau}_i^{\sigma}$ of each UUSV is designed. A Lyapunov function is selected as follows:

$$V_2 = V_1 + \frac{1}{2} z_2^{\mathrm{T}} z_2 + \frac{1}{2} z_3^{\mathrm{T}} z_3 \tag{24}$$

The derivative of V_2 with respect to time is

$$\dot{V}_2 = \dot{V}_1 + z_2^{\mathrm{T}} \dot{z}_2 + z_3^{\mathrm{T}} \dot{z}_3 \tag{25}$$

According to (16), $\dot{z}_2$ can be represented as follows:

$$\dot{z}_2 = -\gamma^{-1} z_2 + \boldsymbol{K}_1 \dot{z}_1 + \boldsymbol{K}_0 \left[1 - \tanh^{\mathrm{T}}\left(\frac{Nz_1}{\varepsilon}\right)\tanh\left(\frac{Nz_1}{\varepsilon}\right)\right]\frac{N\dot{z}_1}{\varepsilon} \tag{26}$$

Let $\boldsymbol{B} = \boldsymbol{K}_1 \dot{z}_1 + \boldsymbol{K}_0 \left[1 - \tanh^{\mathrm{T}}\left(\frac{Nz_1}{\varepsilon}\right)\tanh\left(\frac{Nz_1}{\varepsilon}\right)\right]\frac{N\dot{z}_1}{\varepsilon}$, $\boldsymbol{B}$ consist of bounded functions, so there is a positive constant $\overline{B}$ and $\|\boldsymbol{B}\|_2 \leq \overline{B}$.

Equation (25) can be written as

$$\begin{aligned} \dot{V}_2 &= \dot{V}_1 + z_2^{\mathrm{T}}\left(-\gamma^{-1} z_2 + \boldsymbol{B}\right) + z_3^{\mathrm{T}} \dot{z}_3 \\ &= -z_1^{\mathrm{T}}\boldsymbol{K}_1 z_1 - z_2^{\mathrm{T}}\gamma^{-1} z_2 + z_1^{\mathrm{T}} z_2 + z_2^{\mathrm{T}}\boldsymbol{B} + z_3^{\mathrm{T}}\left(z_1 + \dot{z}_3\right) + N\rho_M k_p \varepsilon \end{aligned} \tag{27}$$

According to Lemma 4, the following inequalities can be obtained:

$$z_1^{\mathrm{T}} z_2 \leq \frac{1}{2}(\varepsilon z_1^{\mathrm{T}} z_1 + \frac{1}{\varepsilon} z_2^{\mathrm{T}} z_2) \tag{28}$$

$$z_2^{\mathrm{T}}\boldsymbol{B} \leq \frac{1}{2}(\frac{1}{\varepsilon} z_2^{\mathrm{T}}\boldsymbol{B}^{\boldsymbol{T}}\boldsymbol{B} z_2 + \varepsilon) \tag{29}$$

$\dot{V}_2$ can be written as

$$\begin{aligned} \dot{V}_2 \quad &\leq -\left(\boldsymbol{K}_1 - \tfrac{1}{2}\varepsilon\boldsymbol{I}\right) z_1^{\mathrm{T}} z_1 - z_2^{\mathrm{T}}\left[\gamma^{-1} - \tfrac{1}{2\varepsilon}\left(1 + \boldsymbol{B}^{\boldsymbol{T}}\boldsymbol{B}\right)\boldsymbol{I}\right] z_2 \\ &+ \left(0.5 + N\rho_M k_p\right)\varepsilon + z_3^{\mathrm{T}}\left(z_1 + \dot{z}_3\right) \end{aligned} \tag{30}$$

With $\boldsymbol{B}_1 = z_1 + \dot{z}_3, \boldsymbol{f}_i(\cdot) = \overset{-\sigma}{\boldsymbol{f}_i} + \gamma_i^{-1} z_{i2}$, the following equation can be obtained:

$$z_3^{\mathrm{T}}\boldsymbol{B}_1 = \sum_{i=1}^{N} z_{i3}^{\mathrm{T}}\left[z_{i1} + \frac{1}{m_i^{33}}\boldsymbol{\tau}_i^{\sigma} + \boldsymbol{f}_i(\cdot)\right] \tag{31}$$

$\overset{-\sigma}{\boldsymbol{f}_i}$ is difficult to be accurate. Thus, the RBF neural network is used to process it.

$$\boldsymbol{f}_i(\cdot) = \boldsymbol{W_i} \circ \boldsymbol{h_i} + \varepsilon_i \tag{32}$$

where $\boldsymbol{W}_i = \left[\boldsymbol{W}_{i1}^{\mathrm{T}}, \boldsymbol{W}_{i2}^{\mathrm{T}}, \boldsymbol{W}_{i3}^{\mathrm{T}}\right]^{\mathrm{T}}, \boldsymbol{h}_i = \left[\boldsymbol{h}_{i1}^{\mathrm{T}}, \boldsymbol{h}_{i2}^{\mathrm{T}}, \boldsymbol{h}_{i3}^{\mathrm{T}}\right]^{\mathrm{T}}$, and $\|\varepsilon_i\| \leq \varepsilon_N$, $i = 1, \ldots, N$, $\varepsilon_N > 0$.

$\dot{V}_2$ can be written as

$$\begin{aligned}\dot{V}_2 \quad &\leq -\left(\boldsymbol{K}_1 - \frac{1}{2}\varepsilon\right)\boldsymbol{z}_1^{\mathrm{T}}\boldsymbol{z}_1 - \boldsymbol{z}_2^{\mathrm{T}}\left[\gamma^{-1} - \frac{1}{2\varepsilon}(1+\boldsymbol{B}^{\boldsymbol{T}}\boldsymbol{B})\boldsymbol{I}\right]\boldsymbol{z}_2 + (0.5 + N\rho_M k_p)\varepsilon \\ &+ \sum_{i=1}^{N}\boldsymbol{z}_{i3}^{\mathrm{T}}\left[\boldsymbol{z}_{i1} + \frac{1}{m_i^{33}}\boldsymbol{\tau}_i^{\sigma} + \boldsymbol{W_i} \circ \boldsymbol{h_i} + \varepsilon_i\right]\end{aligned} \tag{33}$$

The attitude control law $\boldsymbol{\tau}_i^{\sigma}$ of each UUSV is designed as follows:

$$\boldsymbol{\tau}_i^{\sigma} = m_i^{33}\left(-\boldsymbol{K}_{i2}\boldsymbol{z}_{i3} - \frac{N\hat{\phi}_i}{2\varepsilon}\boldsymbol{z}_{i3} \circ (\boldsymbol{h_i} \circ \boldsymbol{h_i}) - \boldsymbol{z}_{i1} - \frac{N\hat{b}_{di}}{2\varepsilon}\boldsymbol{z}_{i3}\right) \tag{34}$$

In $\boldsymbol{\tau}_i^{\sigma}$, $\boldsymbol{K}_{i2}$ is a diagonal matrix, where the diagonal element is a positive constant, and the other elements are 0.

Adaptive control law $\dot{\hat{\phi}}_i$ and auxiliary adaptive law $\dot{\hat{b}}_{di}$ based on MLP are as follows:

$$\dot{\hat{\phi}}_i = \Gamma\left\{\frac{N}{2\varepsilon}\sum_{j=1}^{3} z_{i3,j}^2\|\boldsymbol{h}_{ij}\|_2^2 - K_{\phi_i}[\hat{\phi}_i - \hat{\phi}_i(0)]\right\} \tag{35}$$

$$\dot{\hat{b}}_{di} = \Gamma_b\left\{\frac{N}{2\varepsilon}\|\boldsymbol{z}_{i3}\|_2^2 - K_{b_i}[\hat{b}_{di} - \hat{b}_{di}(0)]\right\} \tag{36}$$

where $\phi_i = \|\boldsymbol{W}_{ij}\|_2^2$, $\phi_i > 0$. $\hat{\phi}_i$ is the estimation of ϕ. The initial value of $\hat{\phi}_i$ is $\hat{\phi}_i(0)$. $\widetilde{\phi}_i = \hat{\phi}_i - \phi_i$ is the estimation error. $\Gamma > 0$ is the adaptive gain. $K_{\phi_i} > 0$ is the feedback gain. $\hat{b}_{di}$ is the estimation of $b_{di} = \varepsilon_N + b_d$. $\widetilde{b}_{di} = \hat{b}_{di} - b_{di}$ is the estimation error. Γ_b is the positive adaptive gain. K_{b_i} is the positive feedback gain.

$\dot{V}_2$ can be written as

$$\begin{aligned}\dot{V}_2 \quad &\leq -\left(\boldsymbol{K}_1 - \frac{1}{2}\varepsilon\boldsymbol{I}\right)\boldsymbol{z}_1^{\mathrm{T}}\boldsymbol{z}_1 - \boldsymbol{z}_2^{\mathrm{T}}\left[\gamma^{-1} - \frac{1}{2\varepsilon}(1+\boldsymbol{B}^{\boldsymbol{T}}\boldsymbol{B})\boldsymbol{I}\right]\boldsymbol{z}_2 \\ &- \boldsymbol{z}_3^{\mathrm{T}}\boldsymbol{K}_2\boldsymbol{z}_3 + (0.5 + N\rho_M k_p)\varepsilon \\ &+ \sum_{i=1}^{N}\boldsymbol{z}_{i3}^{\mathrm{T}}\left[\boldsymbol{W_i} \circ \boldsymbol{h_i} - \frac{N}{2\varepsilon}\hat{\phi}_i\boldsymbol{z}_{i3} \circ (\boldsymbol{h_i} \circ \boldsymbol{h_i}) - \frac{N}{2\varepsilon}\hat{b}_{di}\boldsymbol{z}_{i3} + \varepsilon_i\right]\end{aligned} \tag{37}$$

where $\boldsymbol{K}_2 = \mathrm{diag}\{\boldsymbol{K}_{i2}\}$. For the convenience of subsequent discussion, let $\boldsymbol{K}_{\phi} = \mathrm{diag}\{\boldsymbol{K}_{\phi_i}\}$, $\boldsymbol{K}_b = \mathrm{diag}\{\boldsymbol{K}_{b_i}\}$.

Theorem 1. *Under Assumptions 1 and 2, a formation composed of N UUSVs (10) is considered in a directed graph $\mathcal{G}$. The proposed attitude control law (35), MLP-based adaptive control law (36), and auxiliary control law (37) for each UUSV guarantee that the formation system is SGUUB by selecting positive controller parameters $\boldsymbol{K}_0$, $\boldsymbol{K}_1$, $\boldsymbol{K}_2$, $\boldsymbol{K}_{\phi}$, $\boldsymbol{K}_b$, Γ, Γ_b, $\boldsymbol{\gamma}$, ε under bounded initial conditions, where $\boldsymbol{K}_0$, $\boldsymbol{K}_1$, γ satisfy the following conditions:*

$$\lambda(\boldsymbol{K}_0)_{\min} > N^2\rho_M, \lambda_{\min}(\boldsymbol{K}_1) > \frac{1}{2}\varepsilon, \lambda_{\max}(\gamma) < \frac{2\varepsilon}{1+\boldsymbol{B}^{-2}} \tag{38}$$

Let $\boldsymbol{\phi} = [\phi_1, \ldots, \phi_N]^{\mathrm{T}}$, $\hat{\boldsymbol{\phi}} = [\hat{\phi}_1, \ldots, \hat{\phi}_N]^{\mathrm{T}}$, $\hat{\boldsymbol{\phi}}(0) = [\hat{\phi}_1(0), \ldots, \hat{\phi}_N(0)]^{\mathrm{T}}$, $\widetilde{\boldsymbol{\phi}} = [\widetilde{\phi}_1, \ldots, \widetilde{\phi}_N]^{\mathrm{T}}$, $\bar{\boldsymbol{b}}_d = [b_{d1}, \ldots, b_{dN}]^{\mathrm{T}}$, $\hat{\boldsymbol{b}}_d = \left[\hat{b}_{d1}, \ldots, \hat{b}_{dN}\right]^{\mathrm{T}}$, $\tilde{\boldsymbol{b}}_d = \left[\widetilde{b}_{d1}, \ldots, \widetilde{b}_{dN}\right]^{\mathrm{T}}$, and $\hat{\boldsymbol{b}}_d(0) = \left[\hat{b}_{d1}(0), \ldots, \hat{b}_{dN}(0)\right]^{\mathrm{T}}$.

Consider the candidate Lyapunov function V_3 as follows:

$$V_3 = V_2 + \frac{1}{2\Gamma}\widetilde{\boldsymbol{\phi}}^{\mathrm{T}}\widetilde{\boldsymbol{\phi}} + \frac{1}{2\Gamma_b}\widetilde{\boldsymbol{b}}_d^{\mathrm{T}}\widetilde{\boldsymbol{b}}_d \tag{39}$$

The derivative of V_3 with respect to time is

$$\begin{aligned}\dot{V}_3 \quad &= \boldsymbol{B}_2 + \left(0.5 + N\rho_M k_p\right)\varepsilon + \sum_{i=1}^{N}\left\{\begin{array}{l} \boldsymbol{z}_{i3}^{\mathrm{T}}(\boldsymbol{W_i}\circ\boldsymbol{h_i}) - \frac{N}{2\varepsilon}\hat{\phi}_i\boldsymbol{z}_{i3}^{\mathrm{T}}\boldsymbol{z}_{i3}\circ(\boldsymbol{h_i}\circ h_i) \\ +\widetilde{\phi}_i\left(\frac{N}{2\varepsilon}\sum_{j=1}^{3} z_{i3,j}^2\|\boldsymbol{h}_{ij}\|_2^2\right) \\ +\boldsymbol{z}_{i3}^{\mathrm{T}}\left[\varepsilon_i - \frac{N}{2\varepsilon}\hat{b}_{di}\boldsymbol{z}_{i3}\right] + \frac{N}{2\varepsilon}\widetilde{b}_{di}\|\boldsymbol{z}_{i3}\|_2^2 \end{array}\right\} \\ &- \sum_{i=1}^{N}\left\{K_{\phi_i}\widetilde{\phi}_i\left[\hat{\phi}_i - \hat{\phi}_i(0)\right] + K_{b_i}\widetilde{b}_{di}\left[\hat{b}_{di} - \hat{b}_{di}(0)\right]\right\}\end{aligned} \tag{40}$$

Let $\boldsymbol{B}_2 = -\left(\boldsymbol{K}_1 - \frac{1}{2}\varepsilon\boldsymbol{I}\right)\boldsymbol{z}_1^{\mathrm{T}}\boldsymbol{z}_1 - \boldsymbol{z}_2^{\mathrm{T}}\left[\gamma^{-1} - \frac{1}{2\varepsilon}\left(1 + \boldsymbol{B^T B}\right)\boldsymbol{I}\right]\boldsymbol{z}_2 - \boldsymbol{z}_3^{\mathrm{T}}\boldsymbol{K}_2\boldsymbol{z}_3$.
According to Lemma 4, we have

$$z_{i3,j}\boldsymbol{W}_{\boldsymbol{ij}}^{\mathrm{T}}\boldsymbol{h}_{ij} \le \frac{N}{2\varepsilon}\phi_i z_{i3,j}^2\boldsymbol{h}_{\boldsymbol{ij}}^{\mathrm{T}}h_{\boldsymbol{ij}} + \frac{\varepsilon}{2N} \tag{41}$$

It can then be concluded that

$$\boldsymbol{z}_{i3}^{\mathrm{T}}(\boldsymbol{W_i}\circ\boldsymbol{h_i}) = \sum_{j=1}^{3} z_{i3,j}\boldsymbol{W}_{\boldsymbol{ij}}^{\mathrm{T}}\boldsymbol{h_{ij}} \le \frac{N}{2\varepsilon}\phi_i\sum_{j=1}^{3} z_{i3,j}^2\boldsymbol{h}_{\boldsymbol{ij}}^{\mathrm{T}}\boldsymbol{h_{ij}} + \frac{\varepsilon}{2N} \tag{42}$$

$$\frac{N}{2\varepsilon}\hat{\phi}_i\boldsymbol{z}_{i3}^{\mathrm{T}}\boldsymbol{z}_{i3}\circ(\boldsymbol{h_i}\circ\boldsymbol{h_i}) - \frac{N}{2\varepsilon}\widetilde{\phi}_i\left(\sum_{j=1}^{3} z_{i3,j}^2\|\boldsymbol{h_{ij}}\|_2^2\right) = \frac{N}{2\varepsilon}\phi_i\sum_{j=1}^{3} z_{i3,j}^2\boldsymbol{h}_{\boldsymbol{ij}}^{\mathrm{T}}\boldsymbol{h_{ij}} \tag{43}$$

$$\boldsymbol{z}_{i3}^{\mathrm{T}}\left[\varepsilon_i - \frac{N}{2\varepsilon}\hat{b}_{di}\boldsymbol{z}_{i3}\right] \le \|\boldsymbol{z}_{i3}\|_2 b_{di} - \frac{N}{2\varepsilon}\hat{b}_{di}\|\boldsymbol{z}_{i3}\|_2^2 \tag{44}$$

$$\begin{aligned}\boldsymbol{z}_{i3}^{\mathrm{T}}\left[\varepsilon_i - \tfrac{N}{2\varepsilon}\hat{b}_{di}\boldsymbol{z}_{i3}\right] \quad &\le \left(\tfrac{N}{2\varepsilon}\|\boldsymbol{z}_{i3}\|_2^2 + \tfrac{\varepsilon}{2N}\right)b_{di} - \tfrac{N}{2\varepsilon}\hat{b}_{di}\|\boldsymbol{z}_{i3}\|_2^2 \\ &= -\tfrac{N}{2\varepsilon}\widetilde{b}_{di}\|\boldsymbol{z}_{i3}\|_2^2 + \tfrac{\varepsilon}{2N}b_{di}\end{aligned} \tag{45}$$

$\dot{V}_3$ can be written as

$$\dot{V}_3 \le \boldsymbol{B}_2 + \left[\frac{1}{2} + N\rho_M k_p + \frac{1}{2}(\varepsilon_N + b_d)\right]\varepsilon - \sum_{i=1}^{N}\left\{\begin{array}{l} K_{\phi_i}\widetilde{\phi}_i\left[\hat{\phi}_i - \hat{\phi}_i(0)\right] \\ +K_{b_i}\widetilde{b}_{di}\left[\hat{b}_{di} - \hat{b}_{di}(0)\right] \end{array}\right\} \tag{46}$$

According to the following two inequalities,

$$\widetilde{\phi}_i\left[\hat{\phi}_i - \hat{\phi}_i(0)\right] \ge \frac{1}{2}\widetilde{\phi}_i^2 - \frac{1}{2}\left[\phi_i - \hat{\phi}_i(0)\right]^2 \tag{47}$$

$$\widetilde{b}_{di}\left[\hat{b}_{di} - \hat{b}_{di}(0)\right] \ge \frac{1}{2}\widetilde{b}_{di}^2 - \frac{1}{2}\left[b_{di} - \hat{b}_{di}(0)\right]^2 \tag{48}$$

it can further be obtained as

$$\begin{aligned}\dot{V}_3 \leq \boldsymbol{B}_2 \quad &+\left[\frac{1}{2} + N\rho_M k_p + \frac{1}{2}(\varepsilon_N + b_d)\right]\varepsilon - \frac{1}{2}\sum_{i=1}^{N}\left\{K_{\phi_i}\widetilde{\phi}_i^2 + K_{b_i}\widetilde{b}_{di}^2\right\} \\ &+\frac{1}{2}\sum_{i=1}^{N}\left\{K_{\phi_i}\left[\phi_i - \hat{\phi}_i(0)\right]^2 + K_{b_i}\left[b_{di} - \hat{b}_{di}(0)\right]^2\right\} \\ &= -\left(\boldsymbol{K}_1 - \frac{1}{2}\varepsilon\boldsymbol{I}\right)\boldsymbol{z}_1^{\mathrm{T}}\boldsymbol{z}_1 - \boldsymbol{z}_2^{\mathrm{T}}\left[\gamma^{-1} - \frac{1}{2\varepsilon}(1 + \boldsymbol{B}^{\mathrm{T}}\boldsymbol{B})\boldsymbol{I}\right]\boldsymbol{z}_2 - \boldsymbol{z}_3^{\mathrm{T}}\boldsymbol{K}_2\boldsymbol{z}_3 \\ &-\frac{1}{2}\widetilde{\boldsymbol{\phi}}^{\mathrm{T}}\boldsymbol{K}_\phi\widetilde{\boldsymbol{\phi}} - \frac{1}{2}\tilde{\bar{\boldsymbol{b}}}_d^{\mathrm{T}}\boldsymbol{K}_b\tilde{\bar{\boldsymbol{b}}}_d + \frac{1}{2}\left[\boldsymbol{\phi} - \hat{\boldsymbol{\phi}}(0)\right]^{\mathrm{T}}\boldsymbol{K}_\phi\left[\boldsymbol{\phi} - \hat{\boldsymbol{\phi}}(0)\right] \\ &+\frac{1}{2}\left[\bar{\boldsymbol{b}}_d - \hat{\bar{\boldsymbol{b}}}_d(0)\right]^{\mathrm{T}}\boldsymbol{K}_b\left[\bar{\boldsymbol{b}}_d - \hat{\bar{\boldsymbol{b}}}_d(0)\right] \\ &+\left[\frac{1}{2} + N\rho_M k_p + \frac{1}{2}(\varepsilon_N + b_d)\right]\varepsilon\end{aligned} \tag{49}$$

If

$$\begin{aligned}\beta \quad &= \tfrac{1}{2}\left[\boldsymbol{\phi} - \hat{\boldsymbol{\phi}}(0)\right]^{\mathrm{T}}\boldsymbol{K}_\phi\left[\boldsymbol{\phi} - \hat{\boldsymbol{\phi}}(0)\right] + \tfrac{1}{2}\left[\bar{\boldsymbol{b}}_d - \hat{\bar{\boldsymbol{b}}}_d(0)\right]^{\mathrm{T}}\boldsymbol{K}_b\left[\bar{\boldsymbol{b}}_d - \hat{\bar{\boldsymbol{b}}}_d(0)\right] \\ &+\left[\tfrac{1}{2} + N\rho_M k_p + \tfrac{1}{2}(\varepsilon_N + b_d)\right]\varepsilon\end{aligned} \tag{50}$$

we have

$$\begin{aligned}&\dot{V}_3 \leq -\left(\lambda_{\min}(\boldsymbol{K}_1) - \tfrac{1}{2}\varepsilon\right)\boldsymbol{z}_1^{\mathrm{T}}\boldsymbol{z}_1 - \left(\lambda_{\min}\left(\gamma^{-1}\right) - \tfrac{1}{2\varepsilon}\left(1 + \bar{\boldsymbol{B}}^{2}\right)\right)\boldsymbol{z}_2^{\mathrm{T}}\boldsymbol{z}_2 - \lambda_{\min}(\boldsymbol{K}_2)\boldsymbol{z}_3^{\mathrm{T}}\boldsymbol{z}_3 \\ &-\tfrac{1}{2}\lambda_{\min}(\boldsymbol{K}_\phi)\widetilde{\boldsymbol{\phi}}^{\mathrm{T}}\widetilde{\boldsymbol{\phi}} - \tfrac{1}{2}\lambda_{\min}(\boldsymbol{K}_b)\tilde{\bar{\boldsymbol{b}}}_d^{\mathrm{T}}\tilde{\bar{\boldsymbol{b}}}_d + \boldsymbol{\beta}\end{aligned} \tag{51}$$

If

$$\lambda(\boldsymbol{K}_0)_{\min} > N^2\rho_M, \lambda_{\min}(\boldsymbol{K}_1) > \frac{1}{2}\varepsilon, \lambda_{\max}(\gamma) < \frac{2\varepsilon}{1 + \bar{\boldsymbol{B}}^{2}} \tag{52}$$

$\dot{V}_3$ can be written as

$$\dot{V}_3 \leq -\alpha V_3 + \beta \tag{53}$$

where

$$\alpha = \min\left\{\begin{array}{l}[2\lambda_{\min}(\boldsymbol{K}_1) - \varepsilon], \left[2\lambda_{\min}\left(\gamma^{-1}\right) - \frac{1}{\varepsilon}\left(1 + \bar{\boldsymbol{B}}^{2}\right)\right] \\ , 2\lambda_{\min}(\boldsymbol{K}_2), \Gamma\lambda_{\min}(\boldsymbol{K}_\phi), \Gamma_b\lambda_{\min}(\boldsymbol{K}_b)\end{array}\right\} \tag{54}$$

According to Lemma 5, we can conclude that all attitude subsystems are SGUUB.

3.2. Position Controller Design

For the position subsystem, define error variables $\boldsymbol{z}_{i4}$, $\boldsymbol{z}_{i5}$, $\boldsymbol{z}_{i6}$ as follows:

$$\left\{\begin{array}{l}\boldsymbol{z}_{i4} = \sum\limits_{j=1}^{N} a_{ij}\left[(P_i - \Delta_i) - \left(P_j - \Delta_j\right)\right] + d_i(P_i - \Delta_i - P_r) \\ \boldsymbol{z}_{i5} = \overline{\alpha}_{i2} - \alpha_{i2} \\ \boldsymbol{z}_{i6} = U_i - \overline{\alpha}_{i2}\end{array}\right. \tag{55}$$

where α_{i2} is a virtual control law. $\overline{\alpha}_{i2}$ is a filter control law. $\overline{\alpha}_{i2}$ is obtained by α_{i2} through a first-order filter. χ_i is given by the corresponding diagonal element and is a diagonal positive definite matrix.

$$\chi_i\dot{\overline{\alpha}}_{i2}+\overline{\alpha}_{i2}=\alpha_{i2} \tag{56}$$

The derivative of the error variable z_{i4}, z_{i5}, z_{i6} can be obtained by

$$\begin{cases} \dot{z}_{i4}=\sum\limits_{j=1}^{N}a_{ij}\boldsymbol{R}_i(\theta_i)\begin{bmatrix} z_{i5}+z_{i6}+\alpha_{i2}-U_r \\ -(z_{j5}+z_{j6}+\alpha_{j2}-U_r) \end{bmatrix}+d_i\boldsymbol{R}_i(\theta_i)(z_{i5}+z_{i6}+\alpha_{i2}-U_r) \\ \dot{z}_{i5}=-\chi_i^{-1}z_{i5}-\dot{\alpha}_{i2} \\ \dot{z}_{i6}=\dfrac{1}{m_i^{11}}\tau_i^X+\overline{f}_i^X+\chi_i^{-1}z_{i5} \end{cases} \tag{57}$$

where $\dot{z}_4$ is expressed by the Kronecker product as $\dot{z}_4=\mathcal{R}^{\mathrm{T}}(\overline{\mathcal{L}}\otimes\boldsymbol{I}_1)(z_5+z_6+\boldsymbol{\alpha}_2-\boldsymbol{U_r})$, $\mathcal{R}=\mathrm{diag}\{\boldsymbol{R}_i(\theta_i)\}$.

Consider the candidate Lyapunov function V_4 as follows:

$$V_4=\frac{1}{2}z_4^{\mathrm{T}}z_4 \tag{58}$$

The derivative of V_4 with respect to time is

$$\dot{V}_4=z_4^{\mathrm{T}}\left[\mathcal{R}^{\mathrm{T}}(\overline{\mathcal{L}}\otimes\boldsymbol{I})(z_5+z_6+\boldsymbol{\alpha}_2-\boldsymbol{U_r})\right] \tag{59}$$

Construct the virtual control law as

$$\alpha_{i2}=-\boldsymbol{M}_{i1}z_{i4}-\boldsymbol{M}_{i0}\tanh\left(\frac{Nz_{i4}}{\delta}\right) \tag{60}$$

where $\boldsymbol{M}_{i1}$,$\boldsymbol{M}_{i0}\in\mathrm{R}^{3\times3}$ is a diagonal matrix. δ is a variable positive constant. Definition $z_4=[z_{14},\ldots,z_{N4}]^{\mathrm{T}}$, $z_5=[z_{15},\ldots,z_{N5}]^{\mathrm{T}}$, $z_6=[z_{16},\ldots,z_{N6}]^{\mathrm{T}}$, $\boldsymbol{M}_0=\mathrm{diag}\{\boldsymbol{M}_{i0}\}$, $\boldsymbol{M}_1=\mathrm{diag}\{\boldsymbol{M}_{i1}\}$, and $\boldsymbol{\chi}=\mathrm{diag}\{\chi_i\}$, $\alpha_2=[\alpha_{i2},\ldots,\alpha_{N2}]^{\mathrm{T}}$.

Therefore, the virtual control law α_{i2} can be written in the following form:

$$\boldsymbol{\alpha}_2=-\boldsymbol{M}_1z_4-\boldsymbol{M}_0\tanh\left(\frac{Nz_4}{\delta}\right) \tag{61}$$

Substituting (61) into (59), we have

$$\begin{aligned} \dot{V}_4=z_4^{\mathrm{T}}\mathcal{R}^{\mathrm{T}}(\overline{\mathcal{L}}\otimes\boldsymbol{I})(z_5+z_6)-z_4^{\mathrm{T}}\mathcal{R}^{\mathrm{T}}(\overline{\mathcal{L}}\otimes\boldsymbol{I})\boldsymbol{M}_1z_4 \\ -\boldsymbol{M}_0z_4^{\mathrm{T}}\mathcal{R}^{\mathrm{T}}(\overline{\mathcal{L}}\otimes\boldsymbol{I})\tanh\left(\tfrac{Nz_4}{\delta}\right)-z_4^{\mathrm{T}}\mathcal{R}^{\mathrm{T}}(\overline{\mathcal{L}}\otimes\boldsymbol{I}_1)\boldsymbol{U_r} \end{aligned} \tag{62}$$

According to Lemma 3, it can be obtained as

$$\begin{aligned} \dot{V}_4 \quad &\le z_4^{\mathrm{T}}\mathcal{R}^{\mathrm{T}}(\overline{\mathcal{L}}\otimes\boldsymbol{I})(z_5+z_6)-z_4^{\mathrm{T}}\mathcal{R}^{\mathrm{T}}(\overline{\mathcal{L}}\otimes\boldsymbol{I})\boldsymbol{M}_1z_4 \\ &+\|z_4\|_\infty\mathcal{R}^{\mathrm{T}}(\overline{\mathcal{L}}\otimes\boldsymbol{I}_1)N\rho_U-\boldsymbol{M}_0z_4^{\mathrm{T}}\mathcal{R}^{\mathrm{T}}(\overline{\mathcal{L}}\otimes\boldsymbol{I})\tanh\left(\tfrac{Nz_4}{\delta}\right) \\ &\le z_4^{\mathrm{T}}\mathcal{R}^{\mathrm{T}}(\overline{\mathcal{L}}\otimes\boldsymbol{I})(z_5+z_6)-z_4^{\mathrm{T}}\mathcal{R}^{\mathrm{T}}(\overline{\mathcal{L}}\otimes\boldsymbol{I})\boldsymbol{M}_1z_4+N\rho_Uk_{p1}\delta\mathcal{R}^{\mathrm{T}}(\overline{\mathcal{L}}\otimes\boldsymbol{I}_1) \\ &+N^2\rho_Uz_4^{\mathrm{T}}\mathcal{R}^{\mathrm{T}}(\overline{\mathcal{L}}\otimes\boldsymbol{I}_1)\tan\mathrm{h}(\tfrac{Nz_4}{\delta})-\boldsymbol{M}_0z_4^{\mathrm{T}}\mathcal{R}^{\mathrm{T}}(\overline{\mathcal{L}}\otimes\boldsymbol{I})\tanh\left(\tfrac{Nz_4}{\delta}\right) \end{aligned} \tag{63}$$

Let $\lambda(\boldsymbol{M}_0)_{\min} > N^2\rho_U$, and we can further conclude that $N^2\rho_Uz_4^T\mathcal{R}^{\mathrm{T}}(\overline{\mathcal{L}}\otimes\boldsymbol{I}_1)\tan\mathrm{h}(\frac{Nz_4}{\delta})-\boldsymbol{M}_0z_4^T\mathcal{R}^{\mathrm{T}}(\overline{\mathcal{L}}\otimes\boldsymbol{I})\tanh\left(\frac{Nz_4}{\delta}\right)<0$.

Further, we have

$$\dot{V}_4\le-z_4^{\mathrm{T}}\mathcal{R}^{\mathrm{T}}(\overline{\mathcal{L}}\otimes\boldsymbol{I})\boldsymbol{M}_1z_4+z_4^{\mathrm{T}}\mathcal{R}^{\mathrm{T}}(\overline{\mathcal{L}}\otimes\boldsymbol{I})(z_5+z_6)+N\rho_Uk_{p1}\delta\mathcal{R}^{\mathrm{T}}(\overline{\mathcal{L}}\otimes\boldsymbol{I}_1) \tag{64}$$

Let $s = \mathcal{R}^{\mathrm{T}}\left(\overline{\mathcal{L}} \otimes \boldsymbol{I}\right)$. We have

$$\dot{V}_4 \leq -z_4^{\mathrm{T}}\boldsymbol{s}\boldsymbol{M}_1 z_4 + z_4^{\mathrm{T}}\boldsymbol{s}(z_5 + z_6) + N\rho_U k_{p1}\delta\boldsymbol{s} \tag{65}$$

Next, the attitude control law $\boldsymbol{\tau}_i^X$ of each UUSV is designed. And a Lyapunov function is selected as follows:

$$V_5 = V_4 + \frac{1}{2}z_5^{\mathrm{T}}z_5 + \frac{1}{2}z_6^{\mathrm{T}}z_6 \tag{66}$$

The derivative of V_5 with respect to time is

$$\dot{V}_5 = \dot{V}_4 + z_5^{\mathrm{T}}\dot{z}_5 + z_6^{\mathrm{T}}\dot{z}_6 \tag{67}$$

where $\dot{z}_5$ can be represented as follows:

$$\dot{z}_5 = -\chi^{-1}z_5 + \boldsymbol{M}_1\dot{z}_4 + \boldsymbol{M}_0\left[1 - \tanh^{\mathrm{T}}\left(\frac{Nz_4}{\delta}\right)\tanh\left(\frac{Nz_4}{\delta}\right)\right]\frac{N\dot{z}_4}{\delta} \tag{68}$$

Let $\boldsymbol{C} = \boldsymbol{M}_1\dot{z}_4 + \boldsymbol{M}_0\left[1 - \tanh^{\mathrm{T}}\left(\frac{Nz_4}{\delta}\right)\tanh\left(\frac{Nz_4}{\delta}\right)\right]\frac{N\dot{z}_4}{\delta}$. And there exists a positive constant $\overline{C}$ that satisfies $\|\boldsymbol{C}\|_2 \leq \overline{C}$.

Then, (67) can be written as

$$\dot{V}_5 = -z_4^{\mathrm{T}}\boldsymbol{s}\boldsymbol{M}_1 z_4 + \boldsymbol{s}z_4^{\mathrm{T}}z_5 + z_6^{\mathrm{T}}\left(\boldsymbol{s}z_4 + \dot{z}_6\right) + z_5^{\mathrm{T}}\left(-\chi^{-1}z_5 + \boldsymbol{C}\right) + N\rho_U k_{p1}\delta\boldsymbol{s} \tag{69}$$

According to Lemma 4, the following inequalities can be obtained:

$$z_4^{\mathrm{T}}z_5 \leq \frac{1}{2}(\delta z_4^{\mathrm{T}}z_4 + \frac{1}{\delta}z_5^{\mathrm{T}}z_5) \tag{70}$$

$$z_5^{\mathrm{T}}\boldsymbol{C} \leq \frac{1}{2}\left(\frac{1}{\delta}z_5^{\mathrm{T}}\boldsymbol{C}^{\boldsymbol{T}}\boldsymbol{C}z_5 + \delta\right) \tag{71}$$

$\dot{V}_5$ can be written as

$$\begin{aligned}\dot{V}_5 \quad &\leq -\left(\boldsymbol{s}\boldsymbol{M}_1 - \tfrac{1}{2}\boldsymbol{s}\delta\right)z_4^{\mathrm{T}}z_4 - z_5^{\mathrm{T}}\left[\chi^{-1} + \tfrac{1}{2\delta}\left(1 + \boldsymbol{C}^{\boldsymbol{T}}\boldsymbol{C}\right)\boldsymbol{I}\right]z_5 \\ &+\left(\tfrac{1}{2} + N\rho_U k_{p1}\boldsymbol{s}\right)\delta + z_6^{\mathrm{T}}\left(\boldsymbol{s}z_4 + \dot{z}_6\right)\end{aligned} \tag{72}$$

With $\boldsymbol{C_1} = \boldsymbol{s}z_4 + \dot{z}_6$, $\boldsymbol{F}_i^X(\cdot) = \overset{-X}{\boldsymbol{f}_i} + \chi_i^{-1}z_{i5}$, the following equation can be obtained:

$$z_6^{\mathrm{T}}\boldsymbol{C_1} = \sum_{i=1}^{N} z_{i6}^{\mathrm{T}}\left[sz_{i4} + \frac{1}{m_i^{11}}\tau_i^X + \boldsymbol{F}_i^X(\cdot)\right] \tag{73}$$

$\overset{-X}{\boldsymbol{f}_i}$ is difficult to be accurate. Thus, the RBF neural network is used to process it.

$$\boldsymbol{F}_i^X(\cdot) = \boldsymbol{W}_{\boldsymbol{i}}^X \circ \boldsymbol{h}_{\boldsymbol{i}}^X + \delta_i \tag{74}$$

where $\boldsymbol{W_i} = \left[\boldsymbol{W}_{i4}^{\mathrm{T}}, \boldsymbol{W}_{i5}^{\mathrm{T}}, \boldsymbol{W}_{i6}^{\mathrm{T}}\right]^{\mathrm{T}}$, $\boldsymbol{h}_i = \left[\boldsymbol{h}_{i4}^{\mathrm{T}}, \boldsymbol{h}_{i5}^{\mathrm{T}}, \boldsymbol{h}_{i6}^{\mathrm{T}}\right]^{\mathrm{T}}$, and $\|\delta_i\| \leq \delta_N, i = 1, \ldots, N, \delta_N > 0$.

$\dot{V}_5$ can be written as

$$\begin{aligned}\dot{V}_5 \quad &\leq -\left(\boldsymbol{s}\boldsymbol{M}_1 - \frac{1}{2}\boldsymbol{s}\delta\right)z_4^{\mathrm{T}}z_4 - z_5^{\mathrm{T}}\left[\chi^{-1} + \frac{1}{2\delta}\left(1 + \boldsymbol{C}^{\boldsymbol{T}}\boldsymbol{C}\right)\boldsymbol{I}\right]z_5 \\ &+\left(\frac{1}{2} + N\rho_U k_{p1}\boldsymbol{s}\right)\delta + \sum_{i=1}^{N} z_{i6}^{\mathrm{T}}\left[sz_{i4} + \frac{1}{m_i^{11}}\tau_i^X + \boldsymbol{W}_{\boldsymbol{i}}^X \circ \boldsymbol{h}_{\boldsymbol{i}}^X + \delta_i\right]\end{aligned} \tag{75}$$

The attitude control law $\boldsymbol{\tau}_i^X$ of each UUSV is designed as follows:

$$\boldsymbol{\tau}_i^X = m_i^{11}\left(-\boldsymbol{M}_{i2}\boldsymbol{z}_{i6} - \frac{N\hat{\phi}_i^X}{2\delta}\boldsymbol{z}_{i6} \circ (\boldsymbol{h}_i^X \circ \boldsymbol{h}_i^X) - s\boldsymbol{z}_{i4} - \frac{N\hat{b}_{di}^X}{2\delta}\boldsymbol{z}_{i6}\right) \tag{76}$$

where $\boldsymbol{M}_{i2}$ is a diagonal matrix.

Adaptive control law $\dot{\hat{\phi}}_i^X$ and auxiliary adaptive law $\dot{\hat{b}}_{di}^X$ based on MLP are as follows:

$$\dot{\hat{\phi}}_i^X = \Gamma^X\left\{\frac{N}{2\delta}\sum_{j=1}^{3} z_{i6,j}^2\left\|\boldsymbol{h}_{ij}^X\right\|_2^2 - \boldsymbol{M}_{\phi_i^X}[\hat{\phi}_i^X - \hat{\phi}_i^X(0)]\right\} \tag{77}$$

$$\dot{\hat{b}}_{di}^X = \Gamma_b^X\left\{\frac{N}{2\delta}\|\boldsymbol{z}_{i6}\|_2^2 - \boldsymbol{M}_{b_i^X}[\hat{b}_{di}^X - \hat{b}_{di}^X(0)]\right\} \tag{78}$$

where $\phi_i^X = \|\boldsymbol{W}_{ij}\|_2^2, \phi_i^X > 0$. $\hat{\phi}_i^X$ is the estimation of ϕ^X. $\hat{\phi}_i^X(0)$ is the initial value of $\hat{\phi}_i^X$. $\widetilde{\phi}_i^X = \hat{\phi}_i^X - \phi_i^X$ is the estimation error. $\Gamma^X > 0$ is the adaptive gain. $\boldsymbol{M}_{\phi_i^X} > 0$ is the feedback gain. $\hat{b}_{di}^X$ is the estimation of $b_{di}^X = \delta_N + b_d^X$. $\widetilde{b}_{di}^X = \hat{b}_{di}^X - b_{di}^X$ is the estimation error. Γ_b^X is the positive adaptive gain. $\boldsymbol{M}_{b_i^X}$ is the positive feedback gain.

$\dot{V}_5$ can be written as

$$\begin{aligned}\dot{V}_5 \quad &\leq -\left(s\boldsymbol{M}_1 - \frac{1}{2}s\delta\right)\boldsymbol{z}_4^{\mathrm{T}}\boldsymbol{z}_4 - \boldsymbol{z}_5^{\mathrm{T}}\left[\boldsymbol{\chi}^{-1} + \frac{1}{2\delta}\left(1 + \boldsymbol{C}^T\boldsymbol{C}\right)\boldsymbol{I}\right]\boldsymbol{z}_5 - \boldsymbol{z}_6^{\mathrm{T}}\boldsymbol{M}_2\boldsymbol{z}_6 \\ &+\left(\frac{1}{2} + N\rho_U k_{p1}\boldsymbol{s}\right)\delta + \sum_{i=1}^{N}\boldsymbol{z}_{i6}^{\mathrm{T}}\left[\boldsymbol{W}_i^X \circ \boldsymbol{h}_i^X - \frac{N\hat{\phi}_i^X}{2\delta}\boldsymbol{z}_{i6} \circ (\boldsymbol{h}_i^X \circ \boldsymbol{h}_i^X) - \frac{N\hat{b}_{di}^X}{2\delta}\boldsymbol{z}_{i6} + \delta_i\right]\end{aligned} \tag{79}$$

where $\boldsymbol{M}_2 = \mathrm{diag}\{\boldsymbol{M}_{i2}\}$. For the convenience of subsequent discussion, let $\boldsymbol{M}_{\phi^X} = \mathrm{diag}\left\{\boldsymbol{M}_{\phi_i^X}\right\}$, $\boldsymbol{M}_{b^X} = \mathrm{diag}\left\{\boldsymbol{M}_{b_i^X}\right\}$.

Theorem 2. *Under assumptions 1 and 2, a formation composed of N UUSVs (11) is considered in a directed graph $\mathcal{G}$. The proposed position control law (76), the MLP-based adaptive control law (77), and the auxiliary control law (78) for each UUSV guarantee that the formation system is SGUUB by selecting positive controller parameters $\boldsymbol{M}_0$, $\boldsymbol{M}_1$, $\boldsymbol{M}_2$, $\boldsymbol{M}_{\phi^X}$, $\boldsymbol{M}_{b^X}$, Γ^X, Γ_b^X, $\boldsymbol{\chi}$, δ under bounded initial conditions, where $\boldsymbol{M}_0$, $\boldsymbol{M}_1$, $\boldsymbol{\chi}$ satisfy the following conditions:*

$$\lambda(\boldsymbol{M}_0)_{\min} > N^2\rho_U, \lambda_{\min}(s\boldsymbol{M}_1) > \frac{1}{2}s\delta, \lambda_{\max}(\boldsymbol{\chi}) < \frac{2\delta}{1 + \overline{C}^2} \tag{80}$$

Let $\boldsymbol{\phi}^X = [\phi_1^X, \ldots, \phi_N^X]^{\mathrm{T}}$, $\hat{\boldsymbol{\phi}}^X = [\hat{\phi}_1^X, \ldots, \hat{\phi}_N^X]^{\mathrm{T}}$, $\hat{\boldsymbol{\phi}}^X(0) = [\hat{\phi}_1^X(0), \ldots, \hat{\phi}_N^X(0)]^{\mathrm{T}}$, $\widetilde{\boldsymbol{\phi}}^X = [\widetilde{\phi}_1^X, \ldots, \widetilde{\phi}_N^X]^{\mathrm{T}}$, $\overline{\boldsymbol{b}}_d^X = [b_{d1}^X, \ldots, b_{dN}^X]^{\mathrm{T}}$, $\hat{\overline{\boldsymbol{b}}}_d^X = \left[\hat{b}_{d1}^X, \ldots, \hat{b}_{dN}^X\right]^{\mathrm{T}}$, $\widetilde{\overline{\boldsymbol{b}}}_d^X = \left[\widetilde{b}_{d1}^X, \ldots, \widetilde{b}_{dN}^X\right]^{\mathrm{T}}$, and $\hat{\overline{\boldsymbol{b}}}_d^X(0) = \left[\hat{b}_{d1}^X(0), \ldots, \hat{b}_{dN}^X(0)\right]^{\mathrm{T}}$.

Consider the candidate Lyapunov function V_6 as follows:

$$V_6 = V_5 + \frac{1}{2\Gamma^X}\widetilde{\boldsymbol{\phi}}^{X\mathrm{T}}\widetilde{\boldsymbol{\phi}}^X + \frac{1}{2\Gamma_b^X}\widetilde{\overline{\boldsymbol{b}}}_d^{X\mathrm{T}}\widetilde{\overline{\boldsymbol{b}}}_d^X \tag{81}$$

The derivative of V_6 with respect to time is

$$\dot{V}_6 = \boldsymbol{C}_2 + \left(\frac{1}{2} + N\rho_U k_{p1}\boldsymbol{s}\right)\delta + \sum_{i=1}^{N}\left\{\begin{array}{l} \boldsymbol{z}_{i6}^{\mathrm{T}}\left(\boldsymbol{W}_{\boldsymbol{i}}^{X}\circ\boldsymbol{h}_{\boldsymbol{i}}^{X}\right) - \frac{N\hat{\phi}_i^X}{2\delta}\boldsymbol{z}_{i6}^{\mathrm{T}}\boldsymbol{z}_{i6}\circ\left(\boldsymbol{h}_{\boldsymbol{i}}^{X}\circ\boldsymbol{h}_{\boldsymbol{i}}^{X}\right) \\ +\widetilde{\phi}_i^X\left(\frac{N}{2\delta}\sum_{j=1}^{3} z_{i6,j}^2\left\|\boldsymbol{h}_{\boldsymbol{ij}}^{X}\right\|_2^2\right) \\ +\boldsymbol{z}_{i6}^{\mathrm{T}}\left[\delta_i - \frac{N\hat{b}_{di}^X}{2\delta}\boldsymbol{z}_{i6}\right] + \frac{N}{2\delta}\widetilde{b}_{di}^X\|\boldsymbol{z}_{i6}\|_2^2 \end{array}\right\} - \sum_{i=1}^{N}\left\{M_{\phi_i^X}\widetilde{\phi}_i^X[\hat{\phi}_i^X - \hat{\phi}_i^X(0)] + M_{b_i^X}\widetilde{b}_{di}^X[\hat{b}_{di}^X - \hat{b}_{di}^X(0)]\right\} \tag{82}$$

Let $\boldsymbol{C}_2 = -\left(\boldsymbol{s}\boldsymbol{M}_1 - \frac{1}{2}\boldsymbol{s}\delta\right)\boldsymbol{z}_4^{\mathrm{T}}\boldsymbol{z}_4 - \boldsymbol{z}_5^{\mathrm{T}}\left[\chi^{-1} + \frac{1}{2\delta}\left(1 + \boldsymbol{C}^{\boldsymbol{T}}\boldsymbol{C}\right)\boldsymbol{I}\right]\boldsymbol{z}_5 - \boldsymbol{z}_6^{\mathrm{T}}\boldsymbol{M}_2\boldsymbol{z}_6$. According to Lemma 4, we have

$$\boldsymbol{z}_{i6}^{\mathrm{T}}\left(\boldsymbol{W}_{\boldsymbol{i}}^{X}\circ\boldsymbol{h}_{\boldsymbol{i}}^{X}\right) \le \frac{N}{2\delta}\phi_i^X\sum_{j=1}^{3} z_{i6,j}^2\boldsymbol{h}_{\boldsymbol{ij}}^{X\mathrm{T}}\boldsymbol{h}_{\boldsymbol{ij}}^{X} + \frac{\delta}{2N} \tag{83}$$

$$\frac{N\hat{\phi}_i^X}{2\delta}\boldsymbol{z}_{i6}^{\mathrm{T}}\boldsymbol{z}_{i6}\circ\left(\boldsymbol{h}_{\boldsymbol{i}}^{X}\circ\boldsymbol{h}_{\boldsymbol{i}}^{X}\right) - \widetilde{\phi}_i^X\left(\frac{N}{2\delta}\sum_{j=1}^{3} z_{i6,j}^2\left\|\boldsymbol{h}_{\boldsymbol{ij}}^{X}\right\|_2^2\right) = \frac{N}{2\delta}\phi_i^X\sum_{j=1}^{3} z_{i6,j}^2\boldsymbol{h}_{\boldsymbol{ij}}^{X\mathrm{T}}\boldsymbol{h}_{\boldsymbol{ij}}^{X} \tag{84}$$

$$\boldsymbol{z}_{i6}^{\mathrm{T}}\left[\delta_i - \frac{N\hat{b}_{di}^X}{2\delta}\boldsymbol{z}_{i6}\right] \le \left(\frac{N}{2\delta}\|\boldsymbol{z}_{i6}\|_2^2 + \frac{\delta}{2N}\right)b_{di}^X - \frac{N}{2\delta}\hat{b}_{di}^X\|\boldsymbol{z}_{i6}\|_2^2 = -\frac{N}{2\delta}\widetilde{b}_{di}^X\|\boldsymbol{z}_{i3}\|_2^2 + \frac{\delta}{2N}b_{di}^X \tag{85}$$

$\dot{V}_6$ can be written as

$$\dot{V}_6 \le \boldsymbol{C}_2 + \left(\frac{1}{2} + \frac{1}{2}\left(\delta_N + b_d^X\right) + N\rho_U k_{p1}\boldsymbol{s}\right)\delta - \sum_{i=1}^{N}\left\{\begin{array}{l} M_{\phi_i^X}\widetilde{\phi}_i^X[\hat{\phi}_i^X - \hat{\phi}_i^X(0)] \\ +M_{b_i^X}\widetilde{b}_{di}^X[\hat{b}_{di}^X - \hat{b}_{di}^X(0)] \end{array}\right\} \tag{86}$$

According to the following two inequalities,

$$\widetilde{\phi}_i^X[\hat{\phi}_i^X - \hat{\phi}_i^X(0)] \ge \frac{1}{2}\widetilde{\phi}_i^{X2} - \frac{1}{2}\left[\phi_i^X - \hat{\phi}_i^X(0)\right]^2 \tag{87}$$

$$\widetilde{b}_{di}^X[\hat{b}_{di}^X - \hat{b}_{di}^X(0)] \ge \frac{1}{2}\widetilde{b}_{di}^{X2} - \frac{1}{2}\left[b_{di}^X - \hat{b}_{di}^X(0)\right]^2 \tag{88}$$

Further, it can be obtained

$$\begin{aligned} \dot{V}_6 &\le \boldsymbol{C}_2 + \left(\frac{1}{2} + \frac{1}{2}(\delta_N + b_d^X) + N\rho_U k_{p1}\boldsymbol{s}\right)\delta - \frac{1}{2}\sum_{i=1}^{N}\left\{M_{\phi i^X}\widetilde{\phi}_i^{X2} + M_{b_i^X}\widetilde{b}_{di}^{X2}\right\} \\ &\quad + \frac{1}{2}\sum_{i=1}^{N}\left\{M_{\phi_i^X}\left[\phi_i^X - \hat{\phi}_i^X(0)\right]^2 + M_{b_i^X}\left[b_{di}^X - \hat{b}_{di}^X(0)\right]^2\right\} \\ &= -\left(\boldsymbol{s}\boldsymbol{M}_1 - \frac{1}{2}\boldsymbol{s}\delta\right)\boldsymbol{z}_4^{\mathrm{T}}\boldsymbol{z}_4 - \boldsymbol{z}_5^{\mathrm{T}}\left[\chi^{-1} + \frac{1}{2\delta}\left(1 + \boldsymbol{C}^{\boldsymbol{T}}\boldsymbol{C}\right)\boldsymbol{I}\right]\boldsymbol{z}_5 - \boldsymbol{z}_6^{\mathrm{T}}\boldsymbol{M}_2\boldsymbol{z}_6 \\ &\quad - \frac{1}{2}\widetilde{\boldsymbol{\phi}}_X^{\mathrm{T}}\boldsymbol{M}_{\phi^X}\widetilde{\boldsymbol{\phi}}^X - \frac{1}{2}\widetilde{\boldsymbol{b}}_d^{X\mathrm{T}}\boldsymbol{M}_{b^X}\widetilde{\boldsymbol{b}}_d^{X} + \frac{1}{2}\left[\boldsymbol{\phi}^X - \hat{\boldsymbol{\phi}}^X(0)\right]^{\mathrm{T}}\boldsymbol{M}_{\phi^X}\left[\boldsymbol{\phi}^X - \hat{\boldsymbol{\phi}}^X(0)\right] \\ &\quad + \frac{1}{2}\left[\bar{\boldsymbol{b}}_d^{X} - \hat{\boldsymbol{b}}_d^{X}(0)\right]^{\mathrm{T}}\boldsymbol{M}_{b^X}\left[\bar{\boldsymbol{b}}_d^{X} - \hat{\boldsymbol{b}}_d^{X}(0)\right] \\ &\quad + \left(\frac{1}{2} + \frac{1}{2}(\delta_N + b_d^X) + N\rho_U k_{p1}\boldsymbol{s}\right)\delta \end{aligned} \tag{89}$$

If

$$\beta^X = \tfrac{1}{2}\left[\boldsymbol{\phi}^X - \hat{\boldsymbol{\phi}}^X(0)\right]^{\mathrm{T}} \boldsymbol{M}_{\phi^X}\left[\boldsymbol{\phi}^X - \hat{\boldsymbol{\phi}}^X(0)\right] + \tfrac{1}{2}\left[\overline{\boldsymbol{b}}_d^X - \hat{\overline{\boldsymbol{b}}}_d^X(0)\right]^{\mathrm{T}} \boldsymbol{M}_{b^X}\left[\overline{\boldsymbol{b}}_d^X - \hat{\overline{\boldsymbol{b}}}_d^X(0)\right] + \left(\tfrac{1}{2} + \tfrac{1}{2}(\delta_N + b_d^X) + N\rho_U k_{p1}\boldsymbol{s}\right)\delta \tag{90}$$

we have

$$\begin{aligned}\dot{V}_6 \leq & -\left(\lambda_{\min}(\boldsymbol{sM}_1) - \tfrac{1}{2}\boldsymbol{s}\delta\right)\boldsymbol{z}_4^{\mathrm{T}}\boldsymbol{z}_4 - \left(\lambda_{\min}(\boldsymbol{\chi}^{-1}) - \tfrac{1}{2\delta}\left(1 + \overline{C}^2\right)\right)\boldsymbol{z}_5^{\mathrm{T}}\boldsymbol{z}_5 \\ & -\lambda_{\min}(\boldsymbol{M}_2)\boldsymbol{z}_6^{\mathrm{T}}z_6 - \tfrac{1}{2}\lambda_{\min}\left(\boldsymbol{M}_{\phi^X}\right)\widetilde{\boldsymbol{\phi}}^{X\mathrm{T}}\widetilde{\boldsymbol{\phi}}^X - \tfrac{1}{2}\lambda_{\min}(\boldsymbol{M}_{b^X})\underset{\sim}{\boldsymbol{b}}_d^{X\mathrm{T}}\underset{\sim}{\boldsymbol{b}}_d^X + \boldsymbol{\beta}^X\end{aligned} \tag{91}$$

If

$$\lambda(\boldsymbol{M}_0)_{\min} > N^2\rho_U, \lambda_{\min}(\boldsymbol{sM}_1) > \frac{1}{2}\boldsymbol{s}\delta, \lambda_{\max}(\boldsymbol{\chi}) < \frac{2\delta}{1 + \overline{C}^2} \tag{92}$$

$\dot{V}_6$ can be written as

$$\dot{V}_6 \leq -\alpha^X V_6 + \boldsymbol{\beta}^X \tag{93}$$

where

$$\alpha^X = \min\left\{\begin{array}{l}[2\lambda_{\min}(\boldsymbol{sM}_1) - \boldsymbol{s}\delta], \left[2\lambda_{\min}(\boldsymbol{\chi}^{-1}) - \frac{1}{\delta}\left(1 + \overline{\mathbf{C}}^2\right)\right] \\ , 2\lambda_{\min}(\boldsymbol{M}_2), \Gamma^X\lambda_{\min}\left(\boldsymbol{M}_{\phi^X}\right), \Gamma_b^X\lambda_{\min}(\boldsymbol{M}_{b^X})\end{array}\right\} \tag{94}$$

According to Lemma 5, we can conclude that all position subsystems are SGUUB.

4. Simulation

This section intends to validate the effectiveness of the distributed formation control algorithm proposed in Section 3. For this purpose, numerical simulation is carried out for a formation mission scenario. The parameters are shown in Table 1 [24]. Consider a formation composed of six UUSVs. The initial state of the formation is set as shown in Table 2.

Table 1. Main model parameters of the UUSV.

Parameter	Value	Parameter	Value
m^{11}	25.8	$Y_{v_i\|v_i\|}$	36.2823
m^{22}	33.8	$Y_{v_i\|r_i\|}$	0.805
m^{33}	2.76	N_{r_i}	1.9
X_{u_i}	0.7225	$N_{r_i\|v_i\|}$	−0.08
$X_{u_i\|u_i\|}$	1.3274	$N_{r_i\|r_i\|}$	0.75
Y_{v_i}	0.8612		

Table 2. Initial states of the UUSV formation.

Description	Value
Vehicle 1	$[-20, 30, 0, 0.1, 0.1, 0.1]^{\mathrm{T}}$
Vehicle 2	$[-10, 20, -\pi/4, 0.1, 0.1, 0.1]^{\mathrm{T}}$
Vehicle 3	$[-15, 5, 0, 0.1, 0.1, 0.1]^{\mathrm{T}}$
Vehicle 4	$[-25, 10, 0, 0.1, 0.1, 0.1]^{\mathrm{T}}$
Vehicle 5	$[-10, 5, 0, 0.1, 0.1, 0.1]^{\mathrm{T}}$
Vehicle 6	$[-5, 5, 0, 0.1, 0.1, 0.1]^{\mathrm{T}}$

By using the proposed control law and adaptive law, the simulation results are depicted in Figures 1–4. Figure 1 shows the trajectories of six vehicles on the plane, and it is obvious that the desired formation shape is finally obtained. Using the designed controller, all the closed-loop systems should be SGUUB.

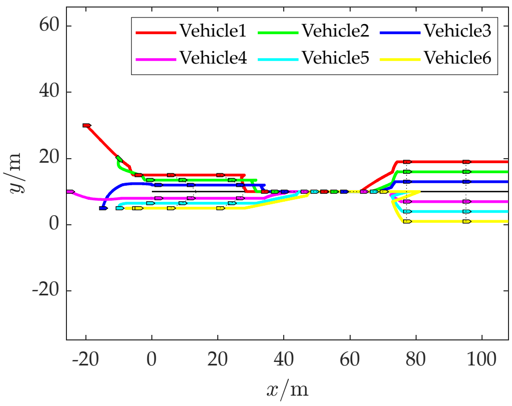

Figure 1. Formation trajectory on plane.

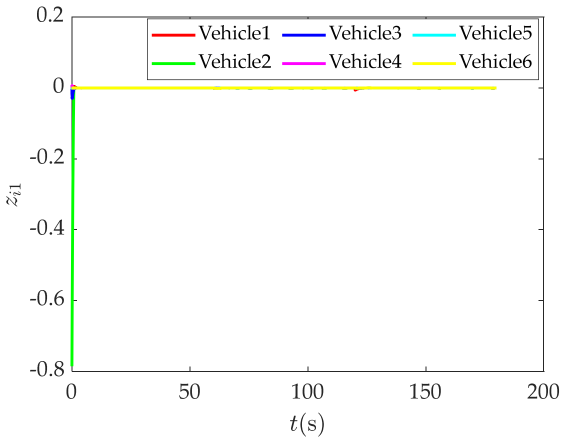

(**a**) Error variable z_{i1}

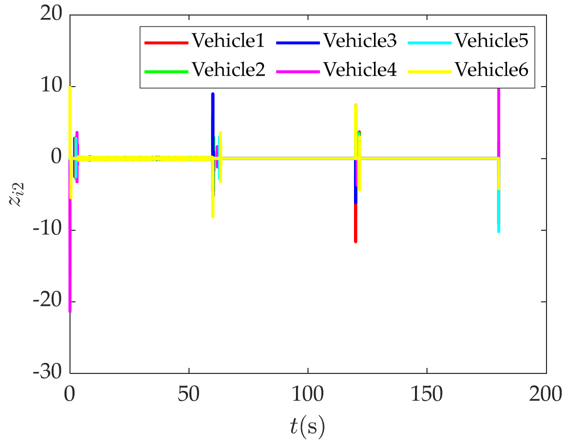

(**b**) Error variable z_{i2}

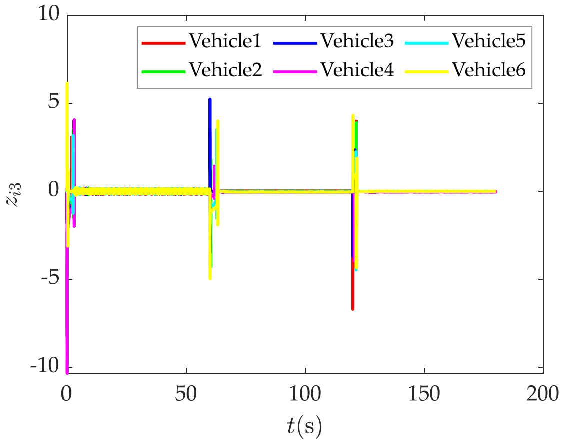

(**c**) Error variable z_{i3}

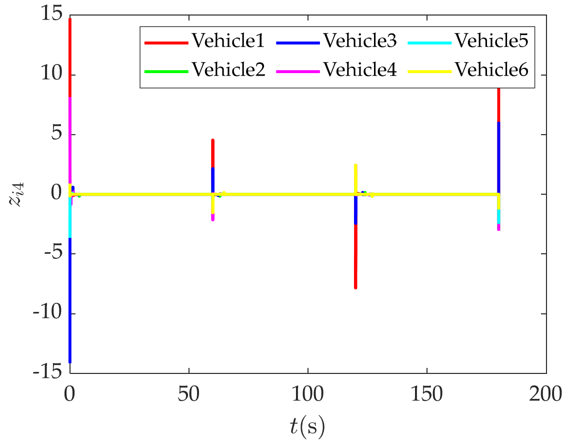

(**d**) Error variable z_{i4}

Figure 2. *Cont.*

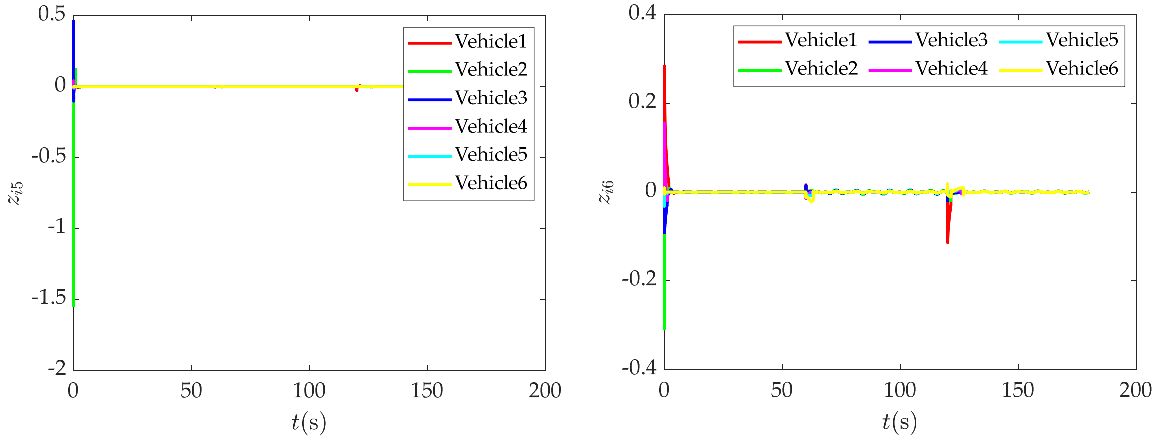

(**e**) Error variable z_{i5} (**f**) Error variable z_{i6}

Figure 2. Model error variables.

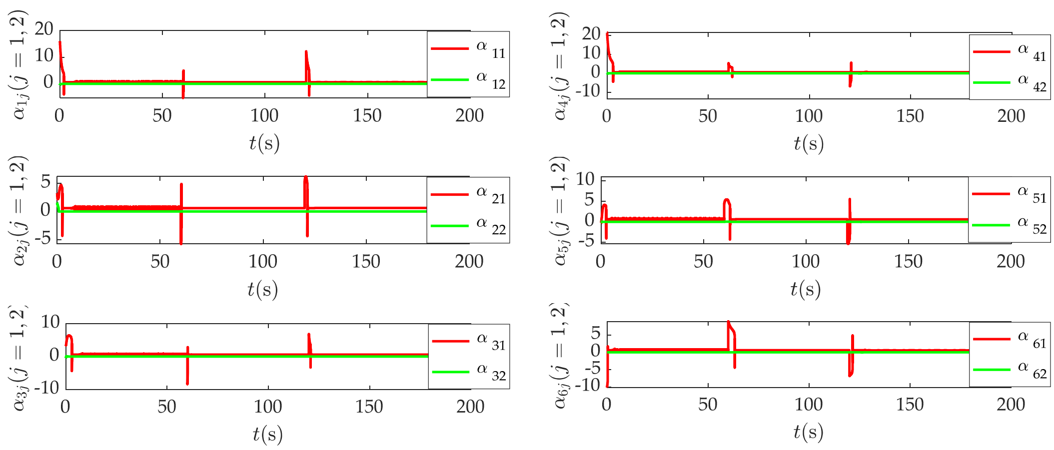

(**a**) Virtual control law $\alpha_{ij}, i=1,2,3, j=1,2$ (**b**) Virtual control law $\alpha_{ij}, i=4,5,6, j=1,2$

Figure 3. Virtual control law.

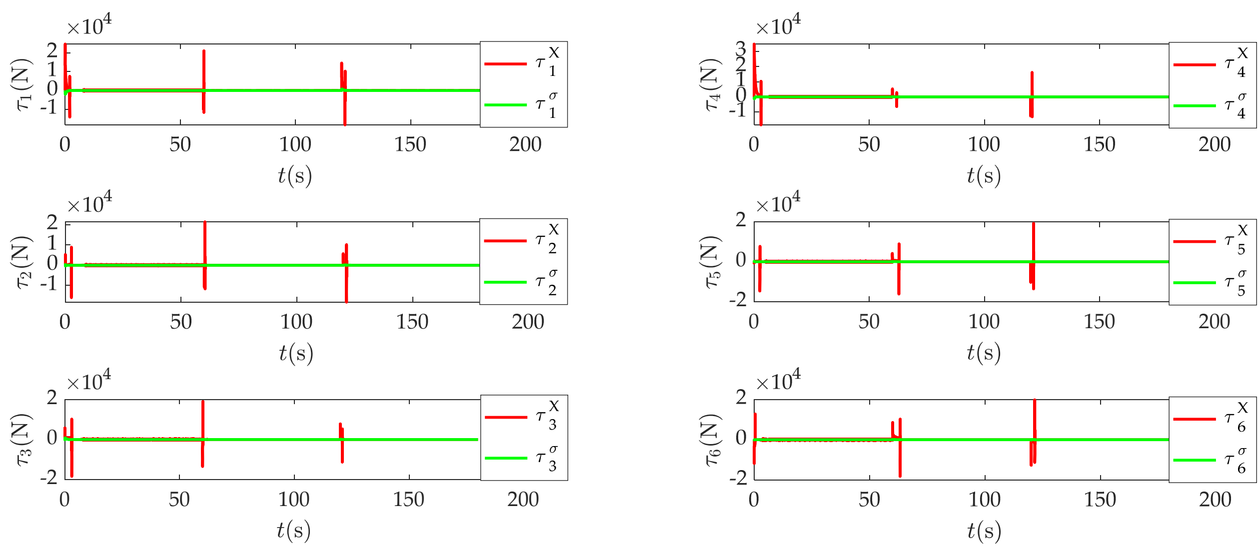

(**a**) Control Input $\tau_i, i=1,2,3$ (**b**) Control Input $\tau_i, i=4,5,6$

Figure 4. Control Input.

Figure 2 shows the error variables of each vehicle. It is obvious that the chattering of the curve is less, and the error variables of the model are SGUUB.

The virtual control laws $\boldsymbol{\alpha}_1$ and $\boldsymbol{\alpha}_2$ of each vehicle are shown in Figure 3. We can observe that the control of the attitude subsystem and the position subsystem are continuous and SGUUB.

The control inputs $\boldsymbol{\tau}^X$ and $\boldsymbol{\tau}^\sigma$ of each vehicle are shown in Figure 4. We can observe that the simulation curve of $\boldsymbol{\tau}^\sigma$ is relatively chattering-free, and all the controls of the position subsystem and attitude subsystem are continuous and SGUUB.

The above simulation results are consistent with Theorems 1 and 2.

5. Conclusions and Discussion

This paper presents a distributed adaptive formation control scheme for UUSV based on a directed graph. In the design process, considering the underactuation characteristics, we redefine the dynamic and kinematic models of the formation. The RBF neural network based on MLP is used for the online approximation of uncertain model parameters and external disturbances. DSC is used to solve the complex differential problem in the calculation process, which further improves the practicability of the controller. From the simulation results, it can be seen that the controller and two adaptive laws designed by this scheme successfully realize the effective control of the formation, achieve the desired goal, and effectively solve the underactuated control of UUSV formation and the uncertain problems of the dynamic model and quantitative parameters. In the future, we will carry out research on the event-triggered UUSV formation control technology.

Author Contributions: Conceptualization, W.H., L.Z. and X.C.; methodology, W.H. and Y.L.; software, W.H.; validation, Y.Z., L.Z. and Y.L.; formal analysis, Y.Z. and W.H.; investigation, L.Z.; resources, L.Z.; data curation, Y.Z.; writing—original draft preparation, W.H.; writing—review and editing, L.Z.; visualization, Y.Z.; supervision, Y.Z.; project administration, L.Z.; funding acquisition, L.Z. All authors have read and agreed to the published version of the manuscript.

Funding: This research was co-funded by the Fundamental Research Funds for the Central Universities grant number 3072024XX0108 and the National Key Research and Development Program of China grant number 2021YFC2803400.

Institutional Review Board Statement: Not applicable.

Informed Consent Statement: Not applicable.

Data Availability Statement: Data are unavailable due to privacy restrictions.

Conflicts of Interest: The authors declare no conflicts of interest.

References

1. Zhang, L.; Zheng, Y.; Huang, B.; Su, Y. Finite-time trajectory tracking control for under-actuated unmanned surface vessels with saturation constraint. *Ocean Eng.* **2022**, *249*, 110745. [CrossRef]
2. Zheng, Y.; Zhang, L. Internal model observer-based distributed moving-target-fencing control of multiple underactuated marine surface vehicles with intermittent communications. *Ocean Eng.* **2024**, *300*, 117383. [CrossRef]
3. Zhang, L.; Zheng, Y.; Huang, Z.; Huang, B.; Su, Y. Distributed global output-feedback formation control without velocity measurement for multiple unmanned surface vehicles. *ISA Trans.* **2024**, *147*, 118–129. [CrossRef] [PubMed]
4. Yan, C.; Zhang, W.; Su, H.; Li, X. Adaptive bipartite time-varying output formation control for multiagent systems on signed directed graphs. *IEEE Trans. Cybern.* **2021**, *52*, 8987–9000. [CrossRef]
5. Wu, W.; Peng, Z.; Wang, D.; Liu, L.; Han, Q.-L. Network-based line-of-sight path tracking of underactuated unmanned surface vehicles with experiment results. *IEEE Trans. Cybern.* **2021**, *52*, 10937–10947. [CrossRef]
6. He, S.; Wang, M.; Dai, S.-L.; Luo, F. Leader–follower formation control of USVs with prescribed performance and collision avoidance. *IEEE Trans. Indust. Informat.* **2018**, *15*, 572–581. [CrossRef]
7. Peng, Z.; Wang, D.; Li, T.; Han, M. Output-feedback cooperative formation maneuvering of autonomous surface vehicles with connectivity preservation and collision avoidance. *IEEE Trans. Cybern.* **2019**, *50*, 2527–2535. [CrossRef]
8. Zheng, Y.; Zhang, L.; Huang, B.; Su, Y. Distributed secure formation control for autonomous surface vessels by performance adjustable event-triggered mechanism. *Int. J. Robust Nonlinear Control* **2023**, *33*, 8490–8507. [CrossRef]

9. Li, S.; Er, M.J.; Wang, N.; Chien, C.-J.; Yang, Z. Adaptive fuzzy output regulation for formation control of unmanned surface vehicles. In Proceedings of the 2017 International Conference on Fuzzy Theory and Its Applications, New York, NY, USA, 12–15 November 2017; pp. 1–6.
10. Peng, Z.; Wang, J.; Wang, D. Distributed maneuvering of autonomous surface vehicles based on neurodynamic optimization and fuzzy approximation. *IEEE Trans. Control Syst. Technol.* **2018**, *26*, 1083–1090. [CrossRef]
11. Peng, Z.; Wang, D.; Chen, Z.; Hu, X.; Lan, W. Adaptive dynamic surface control for formations of autonomous surface vehicles with uncertain dynamics. *IEEE Trans. Control Syst. Technol.* **2012**, *21*, 513–520. [CrossRef]
12. Peng, Z.; Wang, D.; Li, T.; Wu, Z. Leaderless and leader-follower cooperative control of multiple marine surface vehicles with unknown dynamics. *Nonlinear Dyn.* **2013**, *74*, 95–106. [CrossRef]
13. Zhao, Y.; Guo, G.; Ding, L.; Xu, Y.; Xu, H. Collision/obstacle avoidance control of vessel formation. *Inf. Control.* **2012**, *41*, 425–432, 438.
14. He, S.; Dai, S.-L.; Luo, F. Asymptotic trajectory tracking control with guaranteed transient behavior for MSV with uncertain dynamics and external disturbances. *IEEE Trans. Ind. Electron.* **2018**, *66*, 3712–3720. [CrossRef]
15. Chen, Y.; Wei, P. Coordinated adaptive control for coordinated path-following surface vessels with a time-invariant orbital velocity. *IEEE/CAA J. Autom. Sin.* **2014**, *1*, 337–346. [CrossRef]
16. Jin, X. Fault tolerant finite-time leader-follower formation control for autonomous surface vessels with LOS range and angle constraints. *Automatica* **2016**, *68*, 228–236. [CrossRef]
17. Riahifard, A.; Rostami, S.M.H.; Wang, J.; Kim, H.-J. Adaptive leader-follower formation control of under-actuated surface vessels with model uncertainties and input constraints. *Appl. Sci.* **2019**, *9*, 3901. [CrossRef]
18. Qu, Y.; Cai, L. Nonlinear positioning control for underactuated unmanned surface vehicles in the presence of environmental disturbances. *IEEE/ASME Trans. Mechatron.* **2022**, *27*, 5381–5391. [CrossRef]
19. Karnani, C.; Raza, S.A.; Asif, M.; Ilyas, M. Adaptive control algorithm for trajectory tracking of underactuated unmanned surface vehicle (UUSV). *J. Robot.* **2023**, *2023*, 4820479. [CrossRef]
20. Mu, D.; Wang, G.; Fan, Y. Trajectory tracking control for underactuated unmanned surface vehicle subject to uncertain dynamics and input saturation. *Neural Comput. Appl.* **2021**, *33*, 12777–12789. [CrossRef]
21. Li, S.; Wang, X. Finite-time consensus and collision avoidance control algorithms for multiple AUVs. *Automatica* **2013**, *49*, 3359–3367. [CrossRef]
22. Lombana, D.A.B.; Di Bernardo, M. Multiplex PI control for consensus in networks of heterogeneous linear agents. *Automatica* **2016**, *67*, 310–320. [CrossRef]
23. Ge, S.S.; Wang, C. Adaptive neural control of uncertain MIMO nonlinear systems. *IEEE Trans. Neural Netw.* **2004**, *15*, 674–692. [CrossRef] [PubMed]
24. Skjetne, R.; Fossen, T.I.; Kokotović, P.V. Adaptive maneuvering, with experiments, for a model ship in a marine control laboratory. *Automatica* **2005**, *41*, 289–298. [CrossRef]